For office use only		Team Control Number	For office use only	
T1		**44845**	F1	
T2			F2	
T3		Problem Chosen	F3	
T4		**A**	F4	

2016 Mathematical Contest in Modeling (MCM) Summary Sheet

Beneath the Surface: A Thermal-Fluid Analysis of a Hot Bath

The overall temperature and uniformity of heat distribution are crucial to the enjoyment of a hot bath. Over time, a bath will lose heat to its surroundings; however, the temperature can be effectively controlled by adding a trickle of hot water. Quantifying the optimal method of restoring heat uniformly will be the subject of this paper.

By making key assumptions, we reduce the problem to one spatial dimension with three-dimensional heat transfer considerations. We develop three independent, generic mathematical models to describe the temperature distribution of the bathtub in space and time:

- **Steady State, Uniform, Thermodynamic Model:** We characterize the energy and mass interactions between the system and the surroundings, deriving key physical constants used in the subsequent models.
- **Analytical Model**: Using *Fourier analysis* we derive an analytical solution to the one-dimensional heat equation with time dependent Neumann boundary conditions and temporally and spatially dependent heat generation/loss.
- **Numerical Model**: Using a *finite difference approximation* of the one-dimensional convection-diffusion equation, we implement an algorithm that estimates the temperature distribution over time based on bulk fluid motion and diffusion.

We analyze the results of each of these models, performing sensitivity analyses on the input parameters and demonstrating their flexibility. Ultimately, the numerical model proves the most physically accurate as it models convective fluid motion, which is found to dominate thermal diffusion. We then implement *closed-loop PID control* to regulate the total thermal energy of the system. We also model an intelligent strategy for inlet water distribution in order to achieve temperature uniformity.

Ultimately, our model demonstrates that using well-tuned PID control of input water temperature and evenly distributing this water upstream of the bather quickly achieves a uniform objective temperature while conserving water.

Contents

1 Introduction

1.1 Overview

HEAT transfer and fluid flow are notoriously difficult physical mechanisms to accurately model. Over the years, much time and energy has been devoted to obtaining general solutions to these types of problems, but this effort has proven largely unsuccessful. In this paper, we will analyze a specific application of heat transfer and fluid mechanics: modeling the temperature distribution in a bathtub in space and time. The specific scenario is as follows:

Our friend Joseph Fourier (hereafter Joe) decides to take a warm bath and fills his bathtub to the desired temperature. After a while, he notices that the water is cooler than it was initially, and he wishes to increase the temperature by adding a trickle of warm water but does not want to disturb the uniformity of the temperature distribution in space. What should he do to most effectively regain the initial temperature while keeping the temperature uniform throughout and not wasting too much water? What if he wished to eliminate the problem altogether by beginning to add water as soon as he got in the bath?

In this paper, we attempt to answer these questions for Joe. We present our mathematical models describing the temperature distribution in a bathtub in space and time. We describe the relevant physical mechanisms, mathematical development, implementation, and results of each model independently. Then, we compare the results of each model in order to evaluate their accuracy and explore the best solution for Joe. Finally, we present the strengths and weaknesses of our models and discuss ideas for future development of an ideal strategy.

1.2 Nomenclature

We begin by defining a list of nomenclature (symbols) used in this report:

Abbreviation	Description
a	Boundary condition at faucet
b	Boundary condition at overflow drain
c_p	Specific heat
E_{system}	Energy of a system
f	Controls forcing function
g	Gravitational acceleration
Gr_L	Grashof number
h	Enthalpy
h_b	Convection heat transfer coefficient through bottom surface
h_{conv}	Convection heat transfer coefficient
h_t	Convection heat transfer coefficient through top surface
h_w	Convection heat transfer coefficient through the walls
H	Height of bathtub
i	Spatial index variable
j	Temporal index variable

Abbreviation	Description
k	Thermal conductivity
K_d	Derivative gain constant
K_i	Integral gain constant
K_p	Proportional gain constant
L	Length of bathtub
L_c	Characteristic length
m	Mass
n	Summation index variable
Nu	Nusselt number
p	Perimeter
Pe	Péclet number
Pr	Prandtl number
Q	Heat generation
$\tilde{Q}$	Shifted heat generation
Ra_L	Rayleigh number
Re_L	Reynolds number
t	Time
u	Temperature
u_{avg}	Average temperature
u_{in}	Inlet water temperature
u_{obj}	Objective water temperature
u_s	Surface temperature
$\overline{u}$	Difference between average and objective temperature
u_∞	Air temperature
U	Shifted temperature distribution
v	Flow Velocity
W	Width of bathtub
x	Length direction
y	Width direction
z	Height direction
α	Thermal diffusivity
β	Volume expansion coefficient
ϵ	Porosity
η	Fraction of input heat to be redistributed
ν	Kinematic viscosity
σ	Standard deviation from average temperature
ϕ	Initial condition
$\tilde{\phi}$	Shifted initial condition
ρ	Density

1.3 Simplifying Assumptions

All of our models rely on a set of key assumptions that make the problem solvable in a concise manner. The assumptions that are used in every model are summarized below. The additional assumptions for each individual model will be detailed along with the introduction and description of that model.

- The faucet of the bathtub is placed exactly at one end of the length of the bathtub with the overflow drain exactly at the opposite end.
- When Joe is in the bathtub it is full. Any addition of water results immediately in a drainage of the same volume.
- The bathtub is free-standing, i.e. it is surrounded by air on all sides.
- The bathtub itself is in thermal equilibrium with the water at all times. Thus, the interface with the ambient air on all sides can be described without a separate knowledge of the temperature distribution within the bathtub material or the heat capacity of the bathtub.
- All radiation effects are ignored. The only mechanism of stationary heat transfer is convection.
- The ambient air temperature is constant in space and time, i.e. the surroundings can be modeled as a thermal reservoir.
- The ambient air can be modeled as a stationary ideal gas at 1 bar $\approx$ 1 atm.
- No water loss due to evaporation occurs, i.e. the volume of water in the tub remains constant and the surface of the water interacts directly with dry air.
- The presence of the subject in the bathtub provides only thermal effects. There is no disturbance to the flow caused by the subject.
- The flow is uniform, laminar, incompressible, inviscid, and quasi one-dimensional.
- Water has constant density and constant specific heat, and remains in liquid form.
- All material properties are assumed to be isotropic.

As was stated previously, additional assumptions will be described throughout the paper.

2 Geometric Considerations

We begin by defining the geometry of the bathtub. The bathtub will be considered as a rectangular prism, with dimensions equal to L, W, and H as shown below in Figure 1.

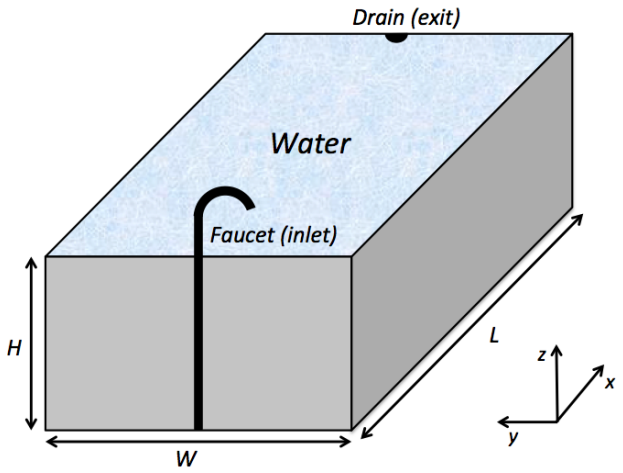

Figure 1: Bathtub Geometry

There are six rectangular faces: five composed of the bathtub material and one face exposed to ambient air. The x direction is taken to be in the length of the bathtub, and y and z describe width and height directions respectively. The faucet is located at $x = 0$ and the drain is located at $x = L$. Any time that we add water to the system through the faucet, an equal volume exits through the overflow drain based on the assumption that the bathtub is full. Physically, modeling the temperature throughout the bathtub is a three-dimensional problem, which complicates the analysis greatly. As we consider partial differential equations (PDEs) with spatial and temporal dependence, simplifying geometric assumptions will be made in order to make the problem more approachable.

The mechanisms of heat transfer and fluid flow within the water will be assumed to be solely in the x direction. The temperature within a cross-section parallel to the yz plane will be assumed to be uniform, and can be thought of as an average temperature over that cross-section. This cross section, with volume $WH\Delta x$, is shown at right.

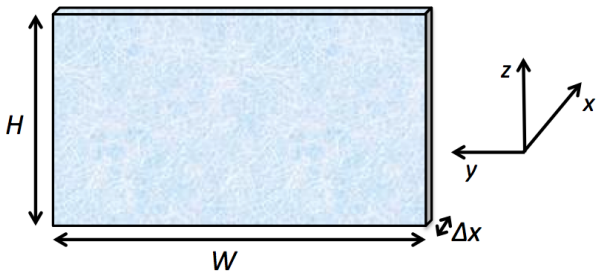

Figure 2: Cross-sectional Fluid Element

These two assumptions allow the three-dimensional problem within the water to be reduced to one dimension. Heat capacity, fluid flow velocity, heat loss to the surroundings, and other *extensive* properties of the system will retain their three dimensional nature, resulting in a final geometric model that is fundamentally one-dimensional, but with important three-dimensional effects preserved. The details of this preservation will be presented along with each individual model development.

3 Thermodynamic Considerations

Next, we examine the key thermodynamic parameters of the problem: the specific enthalpy, specific heat, density, and thermal conductivity of water, as well as the convective heat transfer coefficients from the system to the surrounding air.

3.1 Properties of Water

The specific enthalpy of water is assumed to vary linearly with temperature, with a slope equal to the specific heat. This assumption was validated using property values from the XSteam[1] MATLAB function, shown at right in Figure 3.

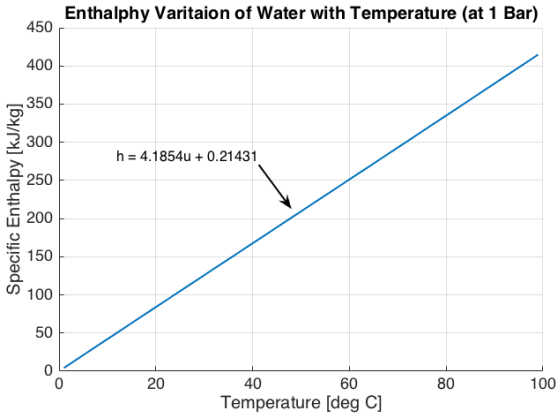

Figure 3: Linear Enthalpy Variation

Mathematically, enthalpy (h) can be calculated from $h = c_p u$, where c_p is the specific heat and u is the temperature. For the purposes of this paper, we will ignore the small y-intercept value and use a constant specific heat[2] of 4178 J/(kgK) based on an assumed average temperature of 30°C.

The density and thermal conductivity of water are taken to be constant at 1000 kg/m^3 and 0.615 W/(mK) respectively[2], based on assumed average temperatures of 30°C.

3.2 Heat Transfer Coefficients

The calculation of convective heat transfer coefficients is involved and will be summarized here. Because the bathtub itself is assumed to be in thermal equilibrium with the water, only convective effects with the surrounding air will be considered. To appropriately estimate the heat transfer coefficient, this convection must be classified as natural (free), forced, or mixed. In particular, we must check the Grashof number (Gr_L) and the Reynolds number (Re_L). If $\mathrm{Gr}_L/\mathrm{Re}_L^2 >> 1$, inertial forces prevail and the natural convection dominates, but if $\mathrm{Gr}_L/\mathrm{Re}_L^2 << 1$, the opposite is true and forced convection dominates. If $\mathrm{Gr}_L/\mathrm{Re}_L^2 \approx 1$, mixed convection must be considered[2].

The formulae for these two dimensionless numbers are shown below, where v is the flow velocity, L is a characteristic length (used in determination of Re_L), ν is the kinematic viscosity of the air, g is the local gravitational acceleration, β is the volume expansion coefficient, u_s and u_∞ are the temperatures of the surface water and air respectively, and L_c is a characteristic length (used in determination of Gr_L)[2].

$$\mathrm{Re}_L = \frac{vL}{\nu} \qquad \mathrm{Gr}_L = \frac{g\beta(u_s - u_\infty)L_c^3}{\nu^2} \tag{1}$$

As a first order approximation, we take $L = 1.5$ m as the length of the bathtub in the flow direction, $\nu = 1.608 \times 10^{-5}$ m^2/s for air at a film temperature of 30°C (a rough estimate of an expected film temperature)[2], $u_s = 40$°C, $u_\infty = 20$°C (rough estimates of the tub and room temperatures respectively), and $g = 9.81$ m/s^2. The flow velocity v is slightly more involved to compute. First, we model the water flowing under the air as air flowing over the water, an equivalent model. Assuming a mass flow rate of 0.06 kg/s (about 1 gallon per minute, a rough estimate of a "trickle"), a bathtub height $H = 0.5$ m, a bathtub width of $W = 1$ m, and uniform, laminar flow from the $x = 0$ face to the $x = L$ face, the flow velocity can be computed as follows:

$$\dot{m} = \rho v A \Rightarrow v = \frac{\dot{m}}{\rho W H} = \frac{0.06 \text{ kg/s}}{(1000 \text{ kg/m}^3)(1 \text{ m})(0.5 \text{ m})} = 1.2 \times 10^{-4} \text{ m/s} \tag{2}$$

For a flat plate of water, $L_c = A_s/p$, the ratio of the surface area to the perimeter[2]. In our case, $L_c = (1.5 \text{ m})(1 \text{ m})/(2(1.5 \text{ m}+1 \text{ m})) = 0.3$ m. Finally, assuming that air is an ideal gas[2], $\beta = 1/T_\infty = 1/293.15 \text{ K} = 0.003411 \text{ K}^{-1}$.

Using these values in the formulae presented in Equation 1, we obtain $\text{Re}_L \approx 11.19$ and $\text{Gr}_L \approx 70000000$. The ratio of interest $\text{Gr}_L/\text{Re}_L^2 \approx 558000 >> 1$, so natural convection effects significantly dominate. Thus, forced convection will be ignored. Even if our rough estimates are slightly incorrect, natural convection should dominate because the ratio is much larger than unity.

Now, we are able to estimate the convective heat transfer coefficients. The determination of these coefficients for a natural convection problem is complicated, but will be summarized briefly here. First, the Rayleigh number must be determined. This number, Ra_L, is the product of the Grashof and Prandtl numbers and describes the ratio of buoyancy forces to thermal and momentum diffusivities. The determination of the Grashof number is shown above, and the Prandtl number, Pr, is a property of the air based on film temperature[2].

Once the Rayleigh number is determined, the Nusselt number, Nu, can be found based on the geometry of the natural convection. In our case, there are six surfaces with three independent geometries. Four of the surfaces (the sides) are modeled as vertical plates, one of the surfaces (the top) is modeled as a flat plate with the hotter side facing up, and one of the surfaces (the bottom) is modeled as a flat plate with the hotter side facing down. Due to the complicated physics of natural convection, these three geometries will have separate heat transfer coefficients. Depending on the magnitude of the Rayleigh number and the geometry, the Nusselt number can be determined as follows[2].

$$\text{Top:} \qquad \text{Nu}_t = \begin{cases} 0.54\text{Ra}_L^{1/4} & 10^4 < \text{Ra}_L < 10^7 \\ 0.15\text{Ra}_L^{1/3} & 10^7 < \text{Ra}_L < 10^{11} \end{cases}$$

$$\text{Bottom:} \qquad \text{Nu}_b = 0.27\text{Ra}_L^{1/4} \quad 10^5 < \text{Ra}_L < 10^{11} \tag{3}$$

$$\text{Wall:} \qquad \text{Nu}_w = \left(0.825 + \frac{0.387\text{Ra}_L^{1/6}}{\left(1 + (0.492/\text{Pr})^{9/16}\right)^{8/27}} \right)^2 \qquad \text{Entire range}$$

At long last, the heat transfer coefficient h_{conv} can be determined from $h_{conv} = \mathrm{Nu}k/L$, where k is the thermal conductivity of the air[2]. In practice, each thermodynamic constant of air is dependent upon the temperature, so there is no explicit solution to these equations. Rather, a system temperature must be guessed and the validity of the guess evaluated. Assuming an air temperature of 20°C, the variation of h_t with water temperature is shown below in Figure 4.

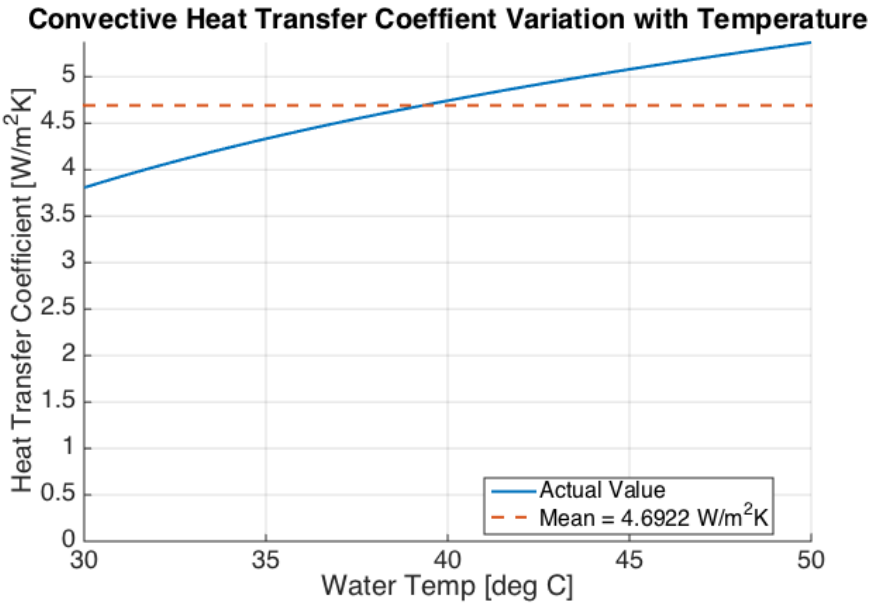

Figure 4: Variation of h_t with Water Temperature

As shown by the above figure, the heat transfer coefficient does vary with temperature of water, as was expected. For the range of temperatures anticipated in the bath water, however, this variation is relatively small. Similarly, the variation of h_b with system temperature is shown below.

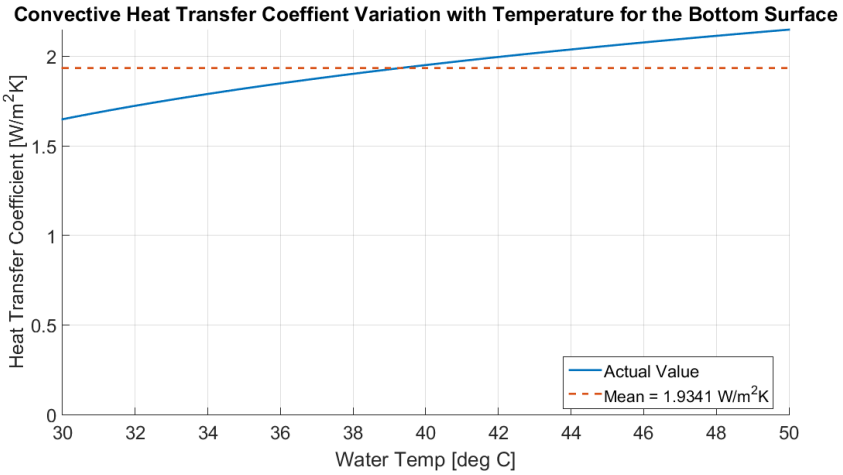

Figure 5: Variation of h_b with Water Temperature

As with h_t, this coefficient varies only slightly with system temperature within expected bounds. It is interesting to note that the magnitude of the coefficient is lower than for the top surface; this is due to the decreased heat loss through natural convection when the hot bathtub is above the colder air. Finally, the same analysis is shown for h_w.

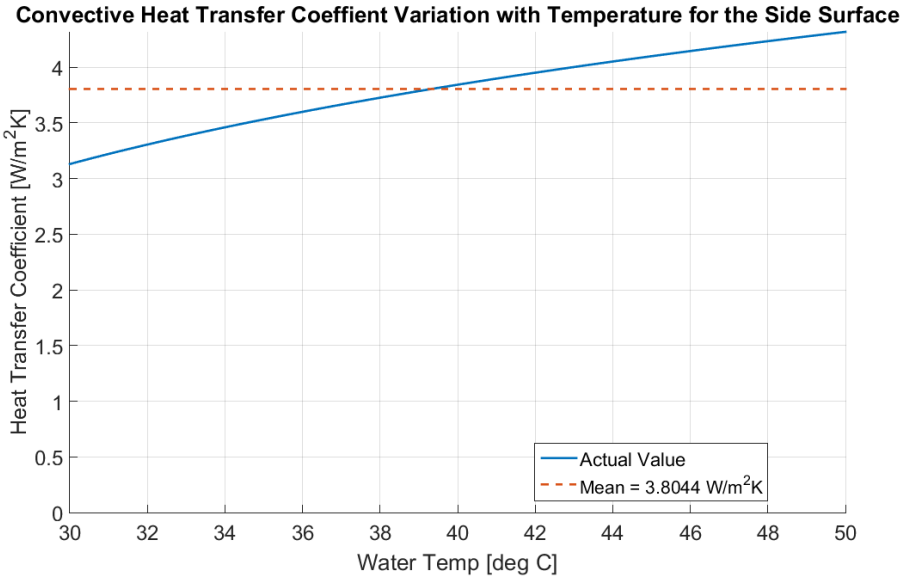

Figure 6: Variation of h_w with Water Temperature

Once again, the coefficient varies only slightly with temperature. The magnitude of the heat transfer coefficient from the walls is between those of the bottom and top surfaces, demonstrating that natural convection is slightly more efficient from vertical walls than from face-down plates, but not as efficient as from face-up plates. In complicated models, it is not realistic to use an iterative numerical method, so the heat transfer coefficients will be taken as their mean value and assumed to not be functions of temperature.

4 Nominal Values Used in Model Simulations

Before describing our first model, we must define the nominal values of each parameter to be used in simulations. In order to conduct reliable analysis of the impact of any one parameter on the solution, we use nominal values of the other parameters. This allows us to examine the effect of a single parameter at a time. The following table contains the model parameters that can be altered as well as their nominal values.

Parameter	Description	Nominal Value
L	Bath Length	1.5 m
W	Bath Width	1 m
H	Bath Height	0.5 m
$\dot{m}$	Mass Flow Rate	0.05 kg/s
u_{in}	Input Water Temp.	45°C
L_{body}	Body Length	1 m
c_{body}	Body Circumference	0.5 m
u_{body}	Body Temperature	37°C
X_{body}	Position of Body Center	0.75 m
h_{body}	Heat Transfer Coeff. of Body	43 W/(m^{2}K) [3]
u_∞	Surroundings Temperature	20°C
u_0	Initial Water Temperature	37°C
k	Thermal Conductivity	0.615 W/(mK) [2]
ρ	Water Density	1000 kg/m^3 [2]
c_p	Specific Heat Capacity	4178 J/(kgK) [2]
h_t	Heat Transfer Coeff. of Top	4.692 W/(m^{2}K)
h_b	Heat Transfer Coeff. of Bottom	1.934 W/(m^{2}K)
h_w	Heat Transfer Coeff. of Wall	3.804 W/(m^{2}K)
t	Time of Bath	1 hr

5 A Steady State, Uniform Temperature Model

5.1 Theory

We now move from defining the geometry and thermodynamic parameters of the problem to developing models for its solution.

As an initial model, the temperature in the bathtub is assumed to be uniform and steady. This allows the analysis to be simply derived from the First Law of Thermodynamics. The *system* will be only the water in the bathtub, and the *surroundings* will be composed of the inlet, the exit, the bather, and the ambient air. This is shown in Figure 7 at right, where the dotted line represents the control volume (the system).

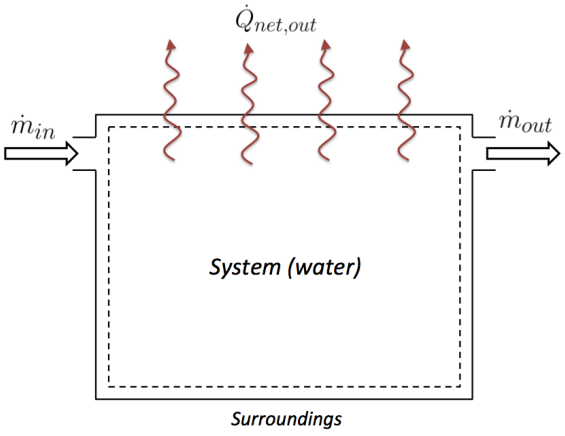

Figure 7: Graphical Illustration of the Thermodynamic System

Assuming steady state, the time derivatives of energy and mass in the system must be zero, as no mass or energy can be accumulating in the system. This is shown mathematically below. The energy equation will be the basis for our model and the mass equation will be used for an important simplification.

$$\frac{dE_{system}}{dt} = 0 \Rightarrow \dot{E}_{in} = \dot{E}_{out} \qquad \frac{dm_{system}}{dt} = 0 \Rightarrow \dot{m}_{in} = \dot{m}_{out} \tag{4}$$

Writing the first equation above using the First Law of Thermodynamics, the following expression can be found[2].

$$\dot{Q}_{in} + \dot{W}_{in} + \sum_{inlets} \dot{m}\left(h + \frac{v^2}{2} + gz\right) = \dot{Q}_{out} + \dot{W}_{out} + \sum_{exits} \dot{m}\left(h + \frac{v^2}{2} + gz\right) \tag{5}$$

Physically, Equation 5 is simply an energy balance. Energy transfer by heat, work, and mass are accounted for with enthalpy, kinetic energy, and potential energy making up the mass transfer terms. We assume only one inlet and one exit, which removes the summation from the equation. We also assume no work done on or by the system, no change in potential energy, and no change in kinetic energy. These are valid assumptions, as the inlet (faucet) and exit (overflow drain) should both be at the level of the water and the kinetic energy terms will be negligible due to the assumed trickle of water. Furthermore, the mass flow entering and leaving should be the same, assuming $\dot{m}_{in} = \dot{m}_{out}$ from Equation 4 above. Finally, we can combine $\dot{Q}_{in}$ and $\dot{Q}_{out}$ into one term representing the net heat transfer. Using these simplifications and the relationship $h = c_p u$, the expression is reduced greatly.

$$\dot{m}c_p u_{in} = \dot{m}c_p u_{out} + \dot{Q}_{net,out} \tag{6}$$

Since we assume uniform temperature distribution, the temperature at the exit is equal to the temperature of the system ($u_{out} = u$). The last piece of this model is to quantify $\dot{Q}_{net,out}$ using the heat transfer coefficients discussed in the previous section. We use Newton's Law of Cooling[2] to find an expression for the convective heat transfer.

$$\dot{Q}_{conv,out} = h_{conv} A(u - u_\infty). \tag{7}$$

Associating the appropriate surface areas with each coefficient, the following expression for the total convective heat loss is found.

$$\dot{Q}_{conv,out} = (u - u_\infty)\left((h_t + h_b)LW + h_w(2HW + 2HL)\right). \tag{8}$$

The presence of Joe in the bathtub provides an additional heat transfer term with its own heat transfer coefficient. We will assume the submerged part of the body is a perfect cylinder without end caps, with a length equal to L_{body}, a circumference of c_{body}, and an external temperature of u_{body}. The total heat loss from the system now includes a term to account for the body and is shown in Equation 9 below.

$$\dot{Q}_{net,out} = (u - u_\infty)\left((h_t + h_b)LW + h_w(2HW + 2HL)\right) + (u - u_{body})h_{body}L_{body}c_{body} \tag{9}$$

By substituting Equation 9 into Equation 6 and solving for u, the final expression for steady, uniform temperature is found.

$$u = \frac{\dot{m}c_p u_{in} + u_\infty\left((h_t + h_b)LW + h_w(2HW + 2HL)\right) + u_{body}h_{body}L_{body}c_{body}}{(h_t + h_b)LW + h_w(2HW + 2HL) + h_{body}L_{body}c_{body}} \tag{10}$$

5.2 Implementation and Results

Equation 10 was implemented using MATLAB. As was discussed previously, the heat transfer coefficients are taken to be averages. Using the nominal parameter values, the steady, uniform temperature as a function of mass flow is shown below in Figure 8.

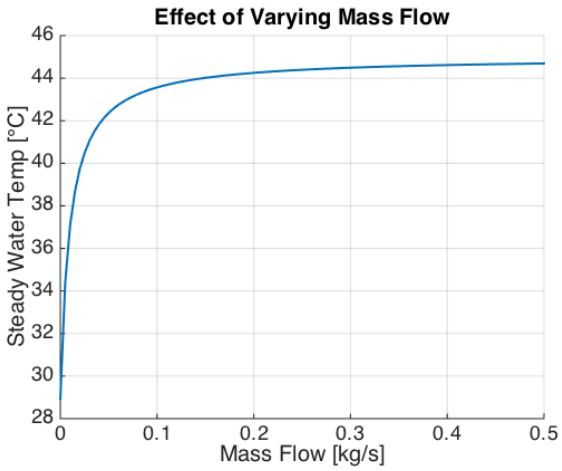

Figure 8: Sensitivity of Final Temperature to Inlet Mass Flow

It is clear from the above figure that increasing the mass flow results in a final temperature that approaches the inlet temperature of 45°C. A similar plot is shown below to illustrate the dependence on inlet temperature.

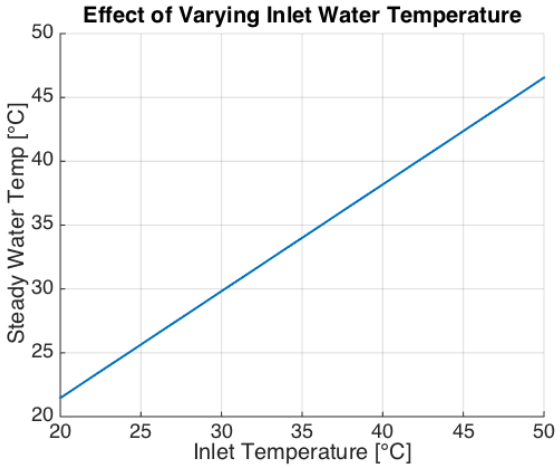

Figure 9: Sensitivity of Final Temperature to Inlet Temperature

When the inlet temperature is close to that of the ambient air (20°C), the steady temperature is higher than that of the inlet, due to the minimal convective heat losses and the effect of the body at 37°C. However, when the inlet temperature is closer to body temperature, the steady temperature is slightly below the inlet temperature due to the increased convective heat losses. Finally, the sensitivity of the solution to ambient air temperature is presented.

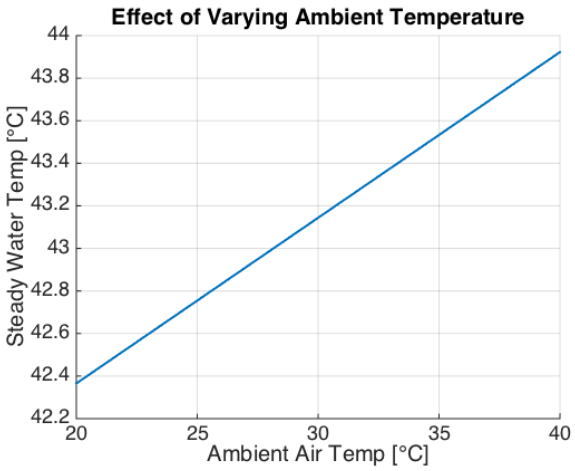

Figure 10: Sensitivity of Final Temperature to Ambient Air Temperature

This model is clearly much less sensitive to this parameter, illustrating minimal heat losses to convection due to the relatively low heat transfer coefficients.

In principle, sensitivities for every parameter could be presented. However, to keep this report concise, we will only present these three. Ultimately, this model is too simple to capture the true dynamical nature of the bathtub system. Thus, more accurate models will be described in the following sections, but the qualitative results here serve as a good baseline for comparison with subsequent models.

6 An Analytical Model of the Heat Equation

In this section, we will describe a model based on an analytical solution to the one-dimensional heat equation with time dependent boundary conditions and time and space dependent heat generation/loss.

6.1 Theory

First, we will derive the analytical solution. The multi-dimensional heat equation with a heat generation term Q is shown below in Equation 11.

$$\frac{\partial u}{\partial t} = \alpha \nabla^2 u + Q(\vec{x}, t) \tag{11}$$

Using the geometric considerations detailed earlier in this report, this PDE can be reduced to one spatial dimension, changing the Laplacian operator to a second partial derivative. The resulting one-dimensional heat equation must be accompanied by an initial condition and boundary conditions in order to fully specify a problem. These conditions, along with the heat generation term, allow our model to effectively describe the physical effects influencing the temperature distribution within the bathtub.

The most appropriate boundary conditions for the bathtub are Neumann conditions which define a heat flux at the boundaries. The heat flux into the tub on the faucet side is

described by the addition of heat to the system, a function of temperature and mass flow of the inlet. The heat flux on the drain side is due to conductive effects through the water at the location of the drain. In order to keep the model generic, these boundary conditions will be allowed to vary with time. The implementation of time dependent boundary conditions allows for greatly increased flexibility and accuracy of the model.

The heat generation term will be extensively used to represent the net effect of both heat loss to the surrounding air and heat generation by Joe himself. As the heat equation admits a heat generation term that is both spatially and temporally dependent, this leads to a highly realistic interpretation of an actual system.

The full presentation of the one dimensional heat equation, with time dependent Neumann boundary conditions, customizable heat source, and initial condition $\phi(x)$, is shown below in Equation 12. Note that subscript notation will be used to represent partial derivatives.

$$\frac{\partial u}{\partial t} = \alpha \frac{\partial^2 u}{\partial x^2} + Q(x,t) \quad , \quad 0 < x < L \quad , \quad t > 0 \quad , \quad \alpha \in \mathbb{R}_{\geq 0} \tag{12}$$

$$\begin{aligned} u_x(x=0,t) &= a(t) \quad , \quad t > 0 \\ u_x(x=L,t) &= b(t) \quad , \quad t > 0 \\ u(x,t=0) &= \phi(x) \quad , \quad 0 < x < L \end{aligned}$$

Unlike many standard PDEs, the method of separation of variables will not yield applicable solutions, due to the inhomogeneity of the forcing function and the time dependence of the boundary conditions. To solve this problem, the method of *shifting the data* will be employed to homogenize the boundary conditions. This method, along with many of the other methods in the following solution, is outlined by Grigoryan[4].

First, we will transform the original equation:

$$u(x,t) = v(x,t) + U(x,t) \qquad \text{where} \qquad U(x,t) = \left(x - \frac{x^2}{2L}\right) a(t) + \frac{x^2}{2L} b(t). \tag{13}$$

Plugging this transformation back into the original PDE, the following transformed PDE, boundary conditions, and initial conditions can be found.

$$\frac{\partial v}{\partial t} - \alpha \frac{\partial^2 v}{\partial x^2} = \tilde{Q}(x,t) \quad , \quad 0 < x < L \quad , \quad t > 0 \quad , \quad \alpha \in \mathbb{R} \tag{14}$$

$$\begin{aligned} v_x(x=0,t) &= 0 \quad , \quad t > 0 \\ v_x(x=L,t) &= 0 \quad , \quad t > 0 \\ v(x,t=0) &= \tilde{\phi}(x) \quad , \quad 0 < x < L \end{aligned}$$

$$\tilde{Q}(x,t) = Q(x,t) - \left(x - \frac{x^2}{2L}\right) \frac{d}{dt}\left(a(t)\right) - \frac{x^2}{2L} \frac{d}{dt}\left(b(t)\right) + \frac{\alpha}{L}\left(b(t) - a(t)\right) \tag{15}$$

$$\tilde{\phi}(x) = \phi(x) - \left(x - \frac{x^2}{2L}\right) a(0) - \frac{x^2}{2L} b(0) \tag{16}$$

The new variable of interest is v, the transformed heat generation is $\tilde{Q}$, the transformed initial condition is $\tilde{\phi}$, and the boundary conditions have been homogenized which was the objective of the transformation.

Now, we apply the principles of Fourier analysis to the PDE to find a general solution for $v(x,t)$. We define $v(x,t)$ as a Fourier series in the spatial dimension. By Fourier's Theorem, this representation is possible for any piecewise smooth v over a finite interval[5].

To be complete, a full linear combination of sines and cosines would be considered, but the presence of two homogeneous Neumann conditions suggests that just a cosine series is sufficient. This cosine series will include a constant term, as Neumann conditions admit a uniform offset. The Fourier series representation of v is shown below in Equation 17, with the Fourier coefficients defined in Equation 18.

$$v(x,t) = \sum_{n=0}^{\infty} v_n(t) \cos\left(\frac{n\pi x}{L}\right) \tag{17}$$

$$v_{n\neq 0}(t) = \frac{2}{L}\int_0^L v(x,t)\cos\left(\frac{n\pi x}{L}\right)dx \qquad v_0(t) = \frac{1}{L}\int_0^L v(x,t)dx \tag{18}$$

Allowing the Fourier coefficients to vary with time is essentially a modification of *variation of parameters*. The same application of Fourier analysis is used on the modified forcing function, as shown below in Equations 19 and 20.

$$\tilde{Q}(x,t) = \sum_{n=0}^{\infty} \tilde{Q}_n(t) \cos\left(\frac{n\pi x}{L}\right) \tag{19}$$

$$\tilde{Q}_{n\neq 0}(t) = \frac{2}{L}\int_0^L \tilde{Q}(x,t)\cos\left(\frac{n\pi x}{L}\right)dx \qquad \tilde{Q}_0(t) = \frac{1}{L}\int_0^L \tilde{Q}(x,t)dx \tag{20}$$

At this point the solution function and the forcing function have been fully defined in terms of their spatial Fourier cosine series. These two Fourier series representations can be substituted into the PDE in Equation 14. After working through the algebra and moving the derivatives into the sums (assuming that they converge), the PDE is reduced to Equation 21.

$$\sum_{n=0}^{\infty}\left[v_n'(t) + \alpha\left(\frac{n\pi}{L}\right)^2 v_n(t)\right]\cos\left(\frac{n\pi x}{L}\right) = \sum_{n=0}^{\infty}\tilde{Q}_n(t)\cos\left(\frac{n\pi x}{L}\right) \tag{21}$$

By equating Fourier coefficients of the above equation, it can be seen that for every nth term of the series, an ordinary differential equation (ODE) in time exists relating the coefficients $v_n(t)$ and $\tilde{Q}_n(t)$. This relationship is shown below in Equation 22.

$$v_n'(t) + \alpha\left(\frac{n\pi}{L}\right)^2 v_n(t) = \tilde{Q}_n(t) \quad , \quad n = 0, 1, 2, \ldots \tag{22}$$

This first order, non-homogeneous ODE with constant coefficients can be solved using the *integrating factor* method in which the full ODE is multiplied by a factor that allows the left side terms to be expressed as a perfect derivative of the product of two functions.

This common process will not be demonstrated here, but the solution is shown in Equation 23 below, where s is a dummy variable of integration.

$$v_n(t) = e^{-\alpha\left(\frac{n\pi}{L}\right)^2 t}\left(v_n(0) + \int_0^t e^{\alpha\left(\frac{n\pi}{L}\right)^2 s}\,\tilde{Q}_n(s)ds\right) \tag{23}$$

Each of these ODEs is for a specific nth term of the Fourier series. Therefore, it is necessary to define the initial condition as a Fourier cosine series, just as was done for the solution variable and the forcing function. The cosine series is shown below in Equation 24, with a note about $v(x,0)$ that will be used in the next step.

$$\tilde{\phi}(x) = \sum_{n=0}^{\infty} \tilde{\phi}_n \cos\left(\frac{n\pi x}{L}\right) \qquad \text{Note: } v(x,0) = \sum_{n=0}^{\infty} v_n(0)\cos\left(\frac{n\pi x}{L}\right) \tag{24}$$

The coefficients are shown in Equation 25.

$$\tilde{\phi}_{n\neq 0} = \frac{2}{L}\int_0^L \tilde{\phi}(x)\cos\left(\frac{n\pi x}{L}\right)dx \qquad \tilde{\phi}_0 = \frac{1}{L}\int_0^L \tilde{\phi}(x)dx \tag{25}$$

By examining the note in Equation 24 and observing that $\tilde{\phi}(x) \equiv v(x,0)$, equating the coefficients results in the relationship $v_n(0) = \tilde{\phi}_n$. Thus,

$$v_{n\neq 0}(0) = \tilde{\phi}_{n\neq 0} \qquad \text{and} \qquad v_0(0) = \tilde{\phi}_0, \tag{26}$$

which can be directly substituted into Equation 23 where $\tilde{\phi}_{n\neq 0}$ and $\tilde{\phi}_0$ are given by Equation 25.

This completes the solution for $v_n(t)$, the Fourier coefficients of the transformed solution. Next, $v(t)$ is represented in terms of these coefficients, where $\tilde{Q}_n$ and $\tilde{\phi}_n$ are the Fourier coefficients of the transformed heat generation and initial condition respectively, both known functions.

$$v(x,t) = \sum_{n=0}^{\infty}\left[\tilde{\phi}_n e^{-\alpha\left(\frac{n\pi}{L}\right)^2 t} + \int_0^t e^{\alpha\left(\frac{n\pi}{L}\right)^2 (s-t)}\tilde{Q}_n(s)ds\right]\cos\left(\frac{n\pi x}{L}\right) \tag{27}$$

A transformation back from v to u by *unshifting the data* completes the solution to the original PDE with time dependent Neumann boundary conditions and time and space dependent heat generation.

$$u(x,t) = \sum_{n=0}^{\infty}\left[\tilde{\phi}_n e^{-\alpha\left(\frac{n\pi}{L}\right)^2 t} + \int_0^t e^{\alpha\left(\frac{n\pi}{L}\right)^2 (s-t)}\tilde{Q}_n(s)ds\right]\cos\left(\frac{n\pi x}{L}\right) + \left(x - \frac{x^2}{2L}\right)a(t) + \frac{x^2}{2L}b(t) \tag{28}$$

This solution is a full analytical model of one-dimensional heat diffusion within the bathtub. It accommodates the effects of time dependent heat flux through the faucet and can account for the effects of Joe's body temperature and convective heat loss to the ambient air, both of which can vary spatially and temporally. The next subsection will detail the implementation of this solution.

6.2 Implementing the Analytical Model

Implementation of the analytical solution is done in MATLAB. Here, we can take full advantage of the underlying vector and matrix structures necessary for these calculations. We define a grid of (x, t) coordinates with grid sizes Δx and Δt.

$$t_{j+1} = t_j + \Delta t \qquad x_{i+1} = x_i + \Delta x \tag{29}$$

Using this grid, Equation 28 is ultimately the addition of $(x \times t)$ matrices, each a product of an $(x \times 1)$ vector and a $(1 \times t)$ vector. The following discussion concerns each term of Equation 28 and its implementation in MATLAB.

To find the coefficients $\tilde{\phi}_n$, the integral in Equation 25 is approximated using a Trapezoidal Rule with a spacing of h and N subdivisions.

$$\int_0^L \tilde{\phi}(x) \cos\left(\frac{n\pi x}{L}\right) dx \approx \frac{h}{2} \sum_{k=1}^{N} \left[\tilde{\phi}(x_{k+1}) \cos\left(\frac{n\pi x_{k+1}}{L}\right) + \tilde{\phi}(x_k) \cos\left(\frac{n\pi x_k}{L}\right)\right] \tag{30}$$

The same approximation is used to compute $\tilde{Q}_n$.

$$\int_0^L \tilde{Q}(x,t) \cos\left(\frac{n\pi x}{L}\right) dx \approx \frac{h}{2} \sum_{k=1}^{N} \left[\tilde{Q}(x_{k+1},t) \cos\left(\frac{n\pi x_{k+1}}{L}\right) + \tilde{Q}(x_k,t) \cos\left(\frac{n\pi x_k}{L}\right)\right] \tag{31}$$

The left-hand side of Equation 31 is a function of t, so the integration on the right-hand side must be performed at every t in the defined grid.

The computation of the time-varying integral in Equation 27 requires more care. A Trapezoidal Rule is still utilized, but the subdivision length becomes a function of time.

$$\int_0^t e^{\alpha\left(\frac{n\pi}{L}\right)^2 (s-t)} \tilde{Q}_n(s) ds \approx \frac{h(t)}{2} \sum_{k=1}^{N} \left[e^{\alpha\left(\frac{n\pi}{L}\right)^2 (s_{k+1}-t)} \tilde{Q}_n(s_{k+1}) + e^{\alpha\left(\frac{n\pi}{L}\right)^2 (s_k-t)} \tilde{Q}_n(s_k)\right] \tag{32}$$

6.3 Basic Results and Verification

The first scenario to simulate is heat loss over time with insulation on both ends of the bathtub. In this scenario, we expect that the heat loss from the bottom, sides, and top of the bathtub will uniformly decrease the temperature of the water over time. The boundary conditions, initial condition, and internal heat generation are modeled in Equation 33.

$$\begin{aligned} u_x(x=0,t) &= 0 \quad , \quad t > 0 \\ u_x(x=L,t) &= 0 \quad , \quad t > 0 \\ u(x,t=0) &= 37\ ^\circ\text{C}, \quad 0 < x < L \\ Q(x,t) &= \tilde{h}(u_\infty - u(x,t-\Delta t)) \quad , \quad 0 < x < L, \quad t > 0 \end{aligned} \tag{33}$$

Physically, $Q(x,t)$ describes the combined heat losses from the water to the tub and surrounding air. The greater the difference between the water temperature and the surrounding air temperature, the greater the heat loss. However, the water temperature is sampled from the previous time step; to reflect this, $t - \Delta t$ is used in place of t when computing the water temperature in space. The coefficient $\tilde{h}$ describes the rate of heat loss through the different surfaces. We expand $\tilde{h}$ in Equation 34.

$$\tilde{h} = \frac{1}{\rho c_p}\left(\frac{2h_w}{W} + \frac{h_b}{H} + \frac{h_t}{H}\right) \tag{34}$$

The subscripts on each h describe the heat transfer coefficients through the wall (h_w), bottom (h_b), and top (h_t). The division of each coefficient by some length indicates the characteristic length relevant to the heat transfer through that surface. In order to have units of °C/s, we divide all terms by the product ρc_p.

With all the relevant data described, the algorithm necessary to compute $u(x,t)$ is to first compute all quantities for $t = 0$. This way, $\tilde{Q}(x,0)$ can be initialized in Equation 35.

$$\tilde{Q}(x,0) = \tilde{h}(u_\infty - \phi(x)) - \left(x - \frac{x^2}{2L}\right)\frac{da(0)}{dt} - \frac{x^2}{2L}\frac{db(0)}{dt} + \frac{\alpha}{L}\big(b(0) - a(0)\big) \tag{35}$$

Now we can iterate over time in a loop. This way, the previous results are used to calculate recursively the heat loss $Q(x,y)$ and then a new $u(x,t)$. Nested in this loop is another loop which iterates over the number of Fourier terms, N. This performs the summation of each Fourier term to yield the final solution. For the data used in Equation 33, Figure 11 displays the temperature distribution in x and t.

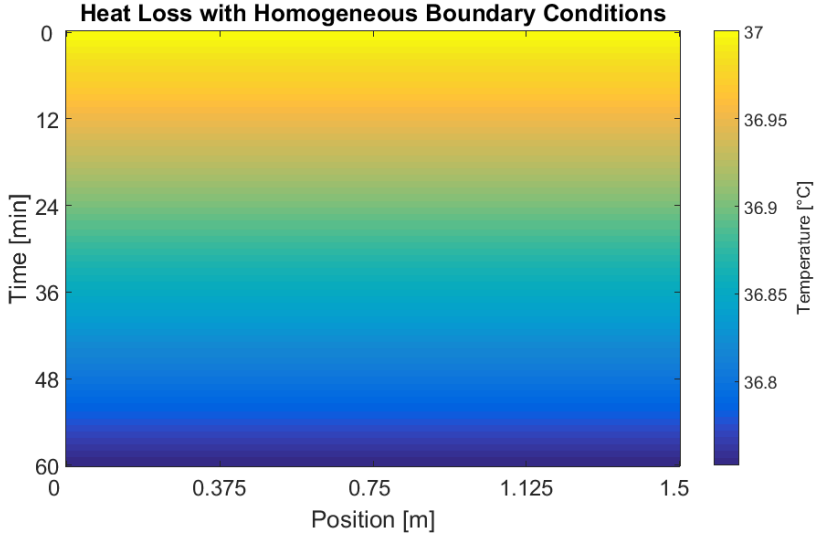

Figure 11: Heat Map of Heat Loss over Time

This result is what we expect: with both ends insulated, the water temperature uniformly decreases over time.

Consider new boundary conditions in Equation 36.

$$
\begin{aligned}
u_x(x=0,t) &= \hat{h}\left[u_{in} - u(0, t-\Delta t)\right] \quad , \quad t>0 \\
u_x(x=L,t) &= \frac{1}{\Delta x}\left[u(L-\Delta x, t-\Delta t) - u(L, t-\Delta t)\right] \quad , \quad t>0 \\
u(x, t=0) &= 37\ ^\circ\text{C}, \quad 0<x<L \\
Q(x,t) &= \tilde{h}[u_\infty - u(x, t-\Delta t)] \quad , \quad 0<x<L, \quad t>0
\end{aligned}
\tag{36}
$$

The boundary condition at $x = 0$ represents an inlet heat flux, entering the system with temperature u_{in}. The boundary condition at $x = L$ is a rough approximation of the heat flux from the previous time step. Similar to the internal heat loss, the heat flux decreases as the water temperature at $x = 0$ approaches u_{in}. The coefficient $\hat{h}$ ensures that the units agree on both sides of the equation. Physically, $\hat{h}$, is proportional to the mass flow rate of water from the inlet. Equation 37 describes this relationship.

$$
\hat{h} = \frac{\dot{m} c_p}{kWH} \tag{37}
$$

The code structure from the previous set of boundary conditions allows for the recursive calculations to compute each new boundary condition. For $u_{in} = 45°\text{C}$, the full solution in x and t for the conditions set in Equation 36 are shown in Figure 12.

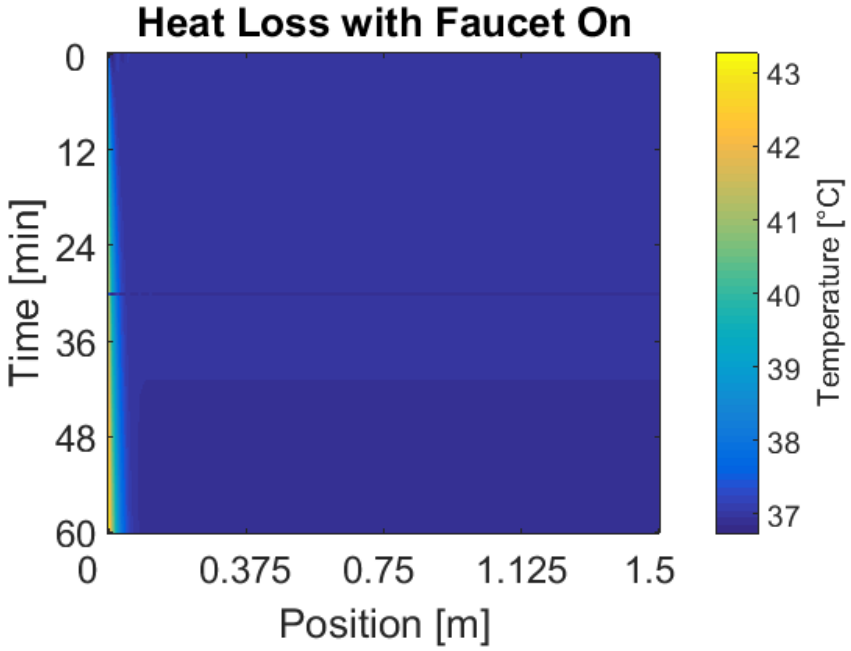

Figure 12: Demonstration of Heat Distribution and Heat Loss With Input Water

Figure 12 demonstrates that the heat propagates through the water. This behavior is expected due to the low thermal diffusivity of water.

Now we simulate a body moving as a point source through the bath. To do so, we define $F(x, t)$.

$$F(x,t) = f \int_{x-t-\epsilon}^{x-t+\epsilon} \delta(x-t-400)d(x-t), \quad 0 < t < 200 \tag{38}$$

Physically, the bather is placed at $x = 400$ at $t = 0$; then, whenever $x = t + 400$, $F(x,t) = f$. f is simply a constant heat generation term defined by the thermodynamic characteristics of the body placed inside the bath. Including in the heat loss term to the surroundings in $Q(x,t)$, our full problem becomes defined as below.

$$\begin{aligned} u_x(x=0,t) &= 0 \quad , \quad t > 0 \\ u_x(x=L,t) &= 0 \quad , \quad t > 0 \\ u(x,t=0) &= 45\ ^\circ\text{C}, \quad 0 < x < L \\ Q(x,t) = F(x,t) + \tilde{h}[u_\infty - u(x,t-\Delta t)] \quad &, \quad 0 < x < L, \quad t > 0 \end{aligned} \tag{39}$$

The new solution is displayed below in Figure 13.

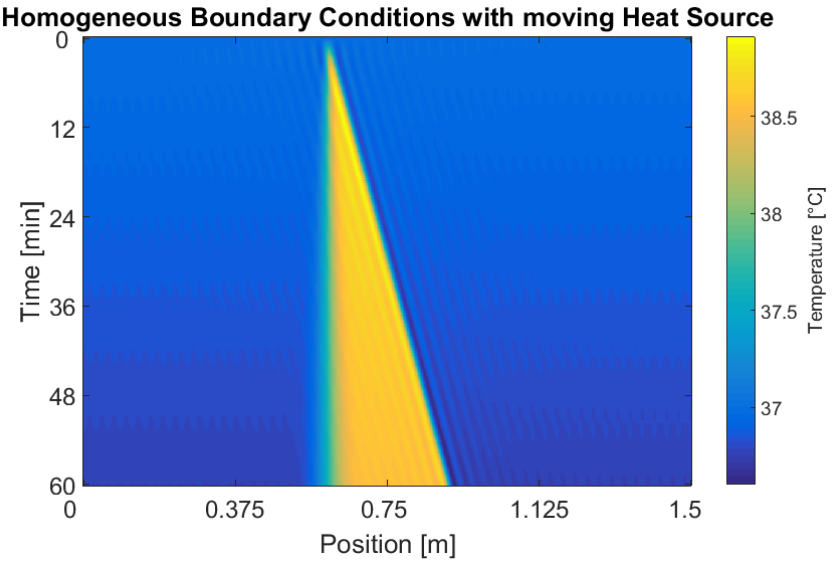

Figure 13: Demonstration of a Moving Heat Source in the Bath

Figure 13 shows that the analytical model is capable of capturing a moving heat source in both space and time. Whenever a point source moves to another location, the previous locations remain at the higher temperature because the heat diffuses very slowly.

7 A Numerical Model of Convection-Diffusion

In this section we will describe our final model: a finite difference approximation of the convection-diffusion equation. We will briefly discuss the theoretical development and implementation, and then present initial results.

7.1 Theory

The problem at hand can be even more effectively modeled as a one-dimensional convection-diffusion problem. The addition of a convection term allows the actual flow of the water – and not just diffusion of heat – to be modeled. It is important to note that convection in this sense means the bulk motion of the water in the tub and not the heat loss to the surroundings. The governing PDE for a convection-diffusion problem is shown below, where the only new quantity is ϵ, the porosity.

$$\frac{\partial u}{\partial t} = \alpha \frac{\partial^2 u}{\partial x^2} - \epsilon v \frac{\partial u}{\partial x} + \frac{q(x,t)}{\rho c_p} \tag{40}$$

In this equation, $\frac{\partial u}{\partial t}$ represents the transient, $\alpha \frac{\partial^2 u}{\partial x^2}$ represents diffusion, $\epsilon v \frac{\partial u}{\partial x}$ represents convection, and the final term represents heat generation or loss. Eliminating the convection and generation terms yields the familiar heat equation presented earlier. Due to the difficulty in solving this equation analytically, a numerical solution will be implemented using the finite difference method, as outlined by Majchrzak and Turcha[6].

The first step is to discretize the temporal and spatial variables, as shown below, where j indexes through time, i indexes through space, and Δt and Δx are the time step and grid spacing, respectively.

$$t_{j+1} = t_j + \Delta t \qquad x_{i+1} = x_i + \Delta x \tag{41}$$

Each derivative can be re-written using a Taylor series in the variable of differentiation. This is shown below in Equation 42, where the superscript represents time indexed in j and the subscript represents space indexed in i.

$$\frac{u_i^j - u_i^{j-1}}{\Delta t} = \alpha \frac{u_{i+1}^j - 2u_i^j + u_{i-1}^j}{(\Delta x)^2} - \epsilon v \frac{u_{i+1}^{j-1} - u_{i-1}^{j-1}}{\Delta x} + \frac{q_i^{j-1}}{\rho c_p} \tag{42}$$

Solving for the temperature at the time (j) and location (i) of interest yields the following numerical solution to the convection-diffusion equation.

$$u_i^j = \left(1 - \frac{2\alpha \Delta t}{(\Delta x)^2}\right) u_i^{j-1} + \left(\frac{\alpha \Delta t}{(\Delta x)^2} + \frac{\epsilon v \Delta t}{2\Delta x}\right) u_{i-1}^{j-1} + \left(\frac{\alpha \Delta t}{(\Delta x)^2} - \frac{\epsilon v \Delta t}{2\Delta x}\right) + \frac{q_i^{j-1}}{c_p \rho} \Delta t \tag{43}$$

When selecting step sizes Δx and Δt, we must ensure that the stability criteria are met since the forward difference approximations are conditionally stable. These criteria are described below.

$$\Delta x < \frac{2\alpha}{\epsilon v}, \quad \Delta t < \frac{(\Delta x)^2}{2\alpha} \tag{44}$$

Should these conditions not be met, the error accumulated in each approximation will grow unboundedly[7].

The final solution, u_i^j, describes the propagation of heat through space and time, and can be implemented in MATLAB. The porosity, ϵ, is the ratio of fluid volume to total volume, and since the medium is entirely fluid, it will be taken as unity. To complete this model, we must now quantify q and enforce appropriate boundary conditions.

The fundamental source of heat transfer in this problem is convection from the water surface and from the bathtub surface. In Equation 43 above, q is the heat transfer per unit volume, where the volume in consideration is a slice of the bathtub in the x direction. This slice has volume $WH\Delta x$. Thus,

$$q = \frac{Q}{WH\Delta x}, \tag{45}$$

where Q is the macroscopic heat loss of the slice. This heat loss is described by the convection terms and the conduction term as follows.

$$Q = (u - u_\infty)(h_t A_t + h_w A_w + h_b A_b) = (u - u_\infty)(h_t(W\Delta x) + h_s(2H\Delta x) + h_b(W\Delta x)) \tag{46}$$

Upon plugging this into Equation 45, we explicitly quantify q due to natural heat transfer effects.

$$q = \frac{(u - u_\infty)}{WH}\left(W(h_t + h_b) + 2Hh_w\right) \tag{47}$$

The same method can be used to model the presence of a person in the bathtub. We estimate that the person will take up a given amount of space in the x direction and have a given circumference c_{body}, which correlates to the exposed area per unit length of the bathtub. The additional heat generation/loss due to the body can be implemented as follows.

$$q_{body} = \frac{h_{body} c_{body}(u - u_{body})}{WH} \tag{48}$$

Together, Equations 47 and 48 make up the heat generation term in the PDE. At a given location i and time step j, we use u_i^{j-1} to estimate u in these equations.

Enforcing the boundary conditions requires some creativity. To enforce the boundary condition on the inlet side, we must specify the correct amount of heat flux into the system as a Neumann condition, increasing the energy content of the fluid element at the boundary based on the mass flow and temperature of the inlet.

The energy entering per unit volume, a q term, can be described as

$$q = \frac{Q}{WH\Delta x} = \frac{\dot{m} c_p (u_{in} - u)}{WH\Delta x}. \tag{49}$$

This can be translated directly into a change in temperature, as in Equation 43 above, by dividing by ρc_p, multiplying by the time step Δt, and approximating u from the previous time step.

$$\Delta u_i^j = \frac{\dot{m}(u_{in} - u_i^{j-1})}{\rho WH\Delta x}\Delta t \tag{50}$$

Equation 50 provides a direct method for changing the temperature of the boundary point in order to account for the heat entering the system.

At the other boundary point, we wish for the water to exit the system naturally, which poses a challenge in prescribing a boundary condition. A realistic condition is that the flux out is equal to the flux between the two points adjacent to the boundary. Thus, the temperature at the end can be specified as follows.

$$u^j_{end} = u^j_{end-1} + \frac{\partial u}{\partial x}\Delta x = u^j_{end-1} + \left(\frac{u^j_{end-1} - u^j_{end-2}}{\Delta x}\right)\Delta x = 2u^j_{end-1} - u^j_{end-2} \tag{51}$$

Now, both boundary conditions have been specified and the finite difference method can be implemented in MATLAB. We will not describe the algorithm here, as it follows directly from the derivation above.

7.2 Basic Results and Verification

In this subsection, we will present some basic results to demonstrate the functionality of our model. First, the problem was modeled with no heat input (the faucet turned off). The results from this simulation are shown below in Figure 14.

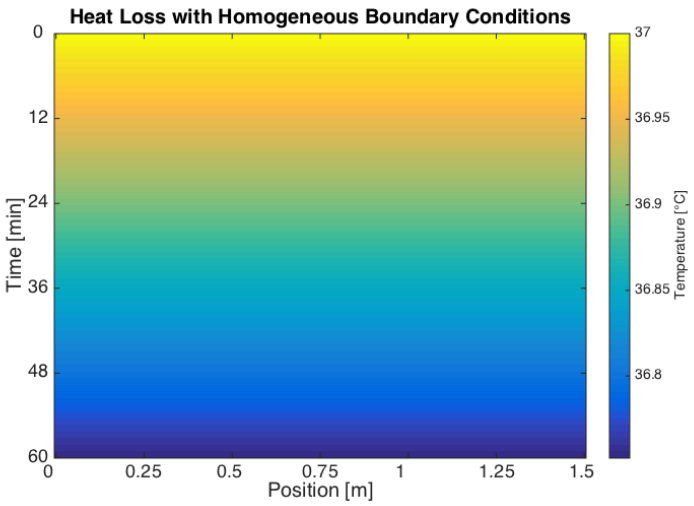

Figure 14: Demonstration of Heat Loss over Time in Numerical Model

The temperature in the tub remains uniform and slowly decreases due to heat loss to the surrounding air. Next, the system was modeled with the faucet on, and the results are shown below.

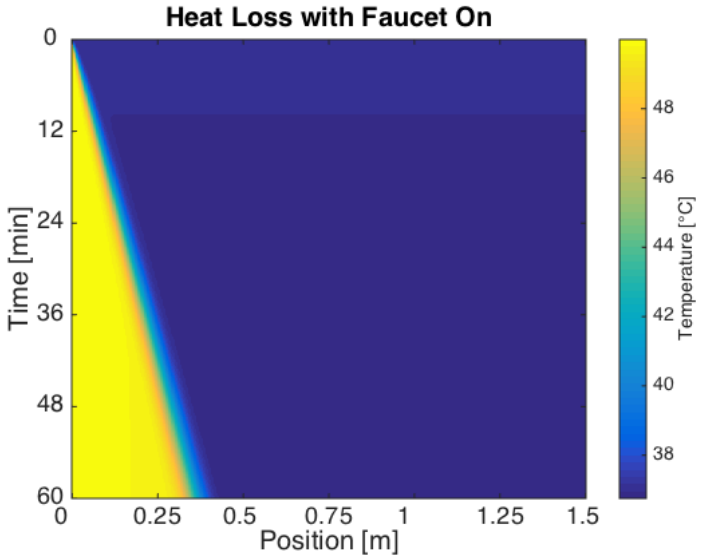

Figure 15: Heat Map of Uniform Mass Flow from Faucet with Heat Loss

This time, the temperature away from the faucet (near $x = L$) drops steadily, as before, but the temperature near the faucet increases to the temperature of the incoming water. Through time, this wave of heat convects through the system at a rate determined by the mass flow and the geometry of the tub. Next, the presence of the bather, Joe, was added and the simulation was run.

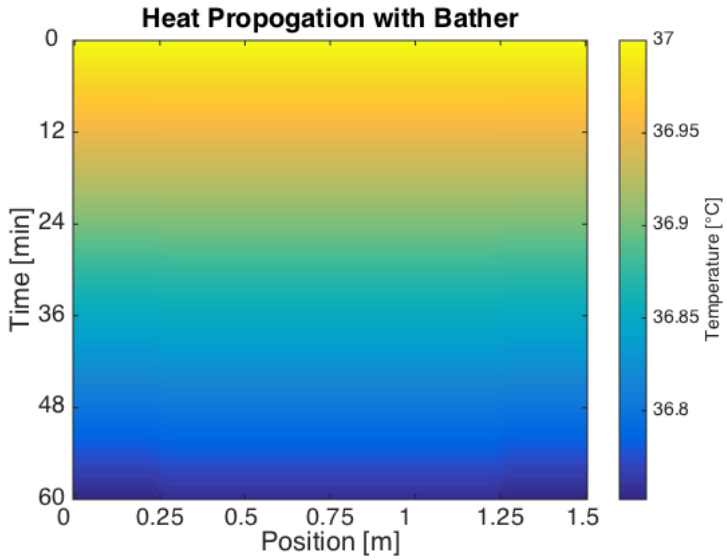

Figure 16: Heat Map of Numerical Model with Bather Present

The deviation of these results from the simulation without the bather is unnoticeable without closely examining the numerical values on a computer. This illustrates that the presence of a bather has little effect on the simulation, an observation that makes physical sense due to the bath temperature and body temperatures being nearly identical.

7.3 Modeling Bather Actions

In this subsection, we will examine the effect of actions of the bather on the solution. As we are assuming no fluid flow other than the bulk, convective motion towards the drain, the bather will have no effect other than to distribute/redistribute heat. Further, we limit ourselves to the case of fixed inlet water temperature and mass flow. This allows the bather to distribute the incoming heat as they wish.

The logic from the boundary condition on the inlet is now extended to the full domain. Given the amount of input energy specified by Equation 49, this energy can be added to any location or combination of locations in the domain, provided that the total amount of energy added to the system does not change from what would have been originally added at the inlet.

This can be implemented by modifying Equation 50, as shown below, where η_i^j (between 0 and 1) is the fraction of available heat prescribed to enter that grid point at that time.

$$\Delta u_i^j = \eta_i^j \frac{\dot{m}(u_{in} - u_i^{j-1})}{\rho W H \Delta x} \Delta t \tag{52}$$

This temperature change term is in addition to the temperature change already calculated from the discretized derivatives and heat loss to the surroundings. In order to conserve energy, the following equality must be defined for all times.

$$\sum_i \eta_i^j = 1 \tag{53}$$

Two interesting applications of bather effects are shown below in Figures 17a and 17b. In the left figure, 99% of the input water was evenly distributed over the whole domain and the remaining 1% was left to trickle through the $x = 0$ boundary. In the right figure, half of the heat was distributed evenly over the region from $x = 0.75$ to $x = 1.5$ and the other half trickled through the faucet.

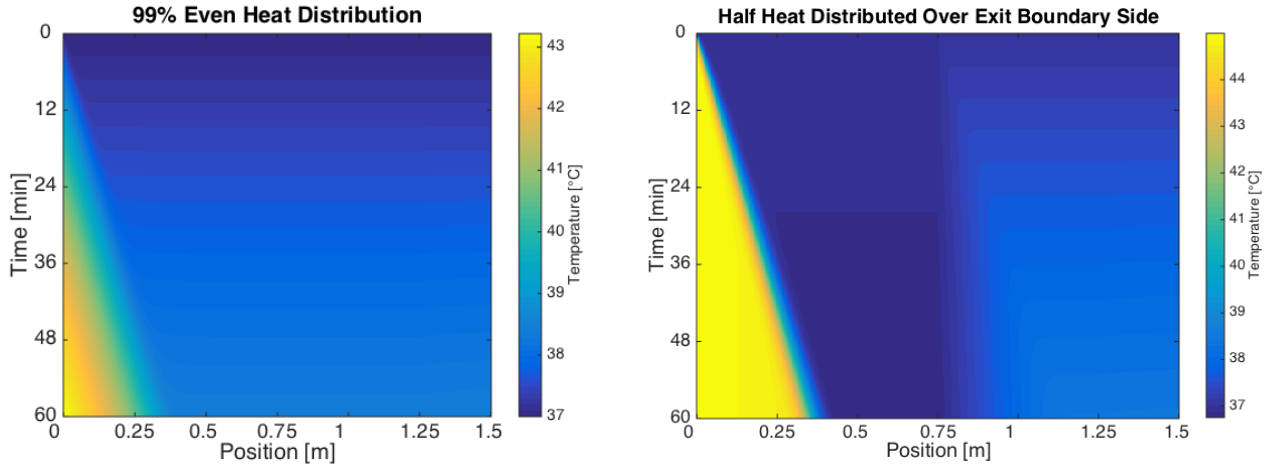

(a) Nearly Uniform Heat Distribution **(b)** Split Heat Distribution

Figure 17: Effects of Redistribution of Water

8 Model Comparison

In this section we present and discuss the major results from both the analytical and numerical models, commenting on the effectiveness and validity of each model.

8.1 Solution Metrics

First, we must develop a metric with which to evaluate our solutions. To do this, we return to the original objective: Joe wishes to attain a desired temperature uniformly distributed throughout the bath. The *desired temperature* constraint and the *uniform distribution* constraint will be decoupled and evaluated separately.

The first metric evaluates the total heat within the bath, addressing the *desired temperature* constraint. This objective function will be called $\overline{u}$, as defined in Equation 54.

$$\overline{u}(t) = u_{avg}(t) - u_{obj} \tag{54}$$

This metric will yield a time-dependent value proportional in magnitude to the difference between the average and objective, with a sign that denotes whether the bath is below or above the objective temperature. As a standard value, the objective temperature of the water will always be a comfortable 37°C.

The second metric quantifies the *uniformity* of the temperature distribution over time. We will define this metric as σ, the standard deviation of the temperature distribution at a given point in time. The equation for the standard deviation is given below in Equation 55.

$$\sigma(t) = \sqrt{\frac{1}{N}\sum_{n=1}^{N}\left(u_n(t) - u_{avg}\right)^2} \tag{55}$$

The evolution of the objective functions (metrics) through time for the numerical model with nominal parameters is shown below, along with the heat map describing the temperature distribution.

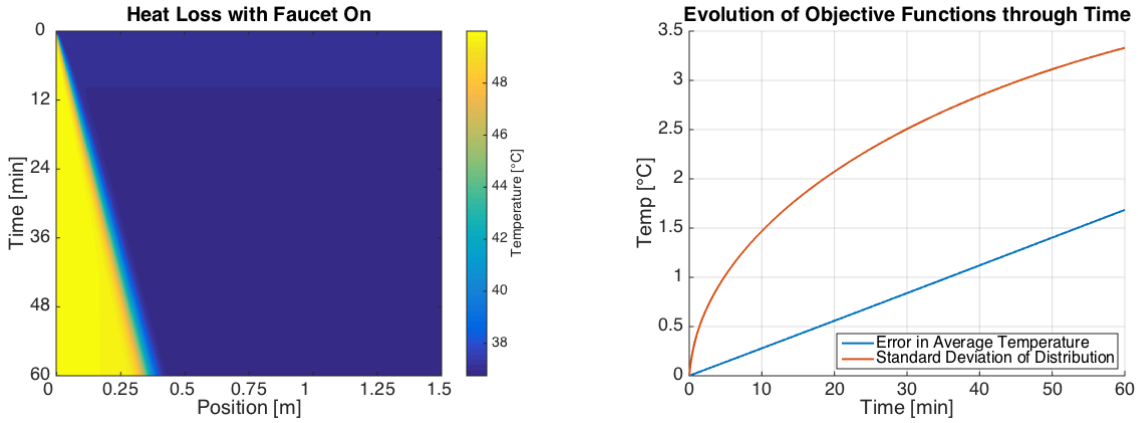

(a) Heat Map of Simulation **(b)** Objective Functions From Simulation

Figure 18: Demonstration of the Objective Functions, $\overline{u}(t)$ and $\sigma(t)$ With Nominal Parameters

By comparing the two plots, the effectiveness of the objective functions is clear; the temperature becomes less uniform as we add too much heat to the system resulting in an increase in the average temperature objective function. In order for Joe to be happy with his bath, our goal is to drive both of these objective functions to zero. As a standard, we will always consider the temperature distribution at the end of a one hour bath. With well defined metrics now in place, simulations can be run to test the impact of each parameter on the solutions from both the analytical and numerical models. The following subsections will each describe the effect of a different parameter on the solution metrics.

8.2 Effect of Bathtub Geometry

The first parameters under consideration are the physical dimensions of the bathtub. Changing the dimensions of the bath changes the surface areas exposed to the air, the velocity of the water flow, and the extensive properties of the fluid element such as mass and volume. Below, we examine the effect of changing the length of the bathtub while holding all other parameters constant.

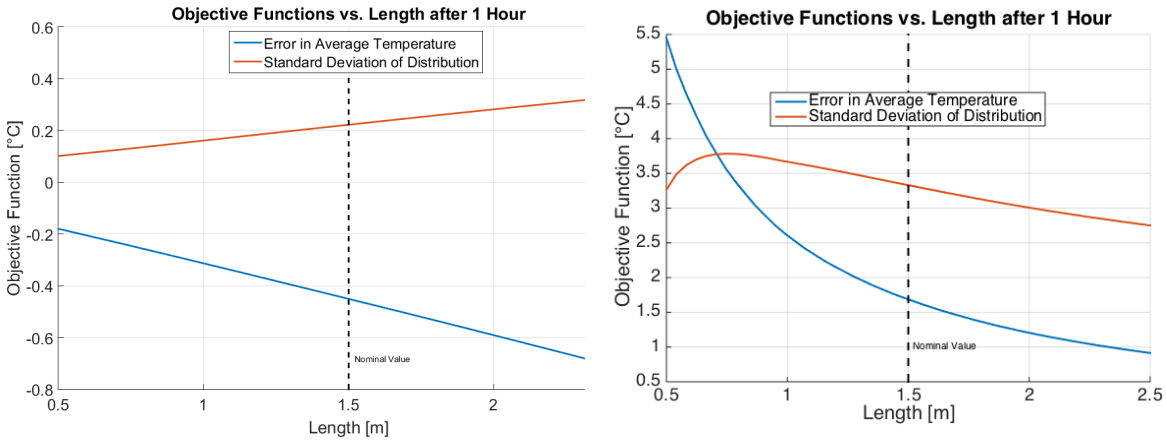

(a) Analytical Model

(b) Numerical Model

Figure 19: Effects of Variation of Length in Both Models

By increasing the length of the bathtub, the error and standard deviation both increase in magnitude for the analytical solution but both decrease in magnitude for the numerical solution which are notably inconsistent results. The analytical model only takes into account the heat diffusion term while the numerical model also accounts for heat convection due to the bulk flow of the water. This fundamental difference is likely the reason for these inconsistent results.

When considering the more accurate numerical model (convection and diffusion) with longer bathtubs, the water is both more uniform and, on average, closer to the objective temperature. As the flow rate is held at its nominal value, a longer bathtub will be less affected by the influx of hot water. The increased error of the analytical model, on the other hand, is due to the low thermal diffusivity of water in comparison to the heat loss of the system. Although hot water is being added to the bath, it cools at a faster rate than the

heat can diffuse through it. Thus, heat builds up at the faucet end of the tub, increasing both error and standard deviation.

A similar study was conducted on the effect of bathtub width, and the results from both models are shown below.

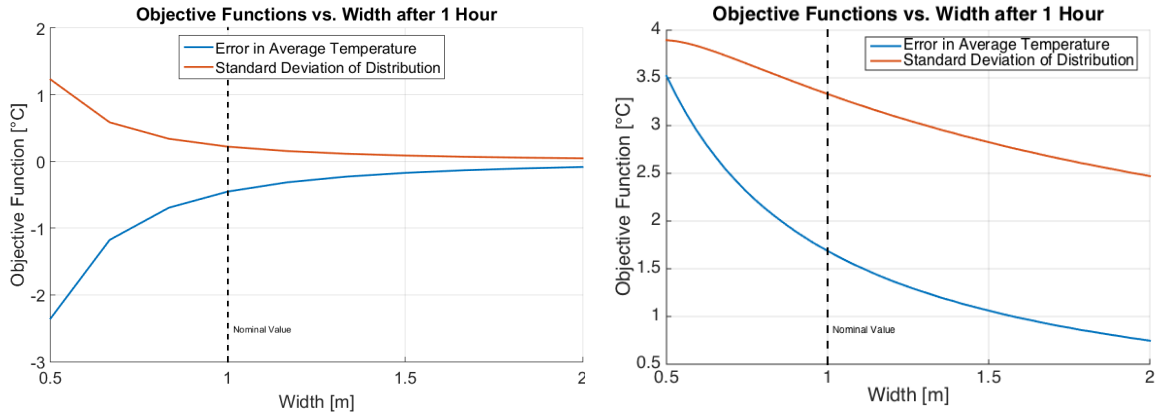

(a) Analytical Model **(b)** Numerical Model

Figure 20: Effects of Variation of Width in Both Models

In this case, the two models qualitatively agree with one another; the temperature error magnitude and the standard deviation are decreasing as width is increased.This result is consistent with the findings of the length variation in the numerical model. The effect of increasing the width is to increase the area exposed to air while maintaining the distance in the direction of diffusion and bulk flow. This increase results in a more uniform temperature distribution as the heat build-up at the inlet is offset by increased heat loss.

Next, the height dimension was varied and the results from the sensitivity analysis are presented below.

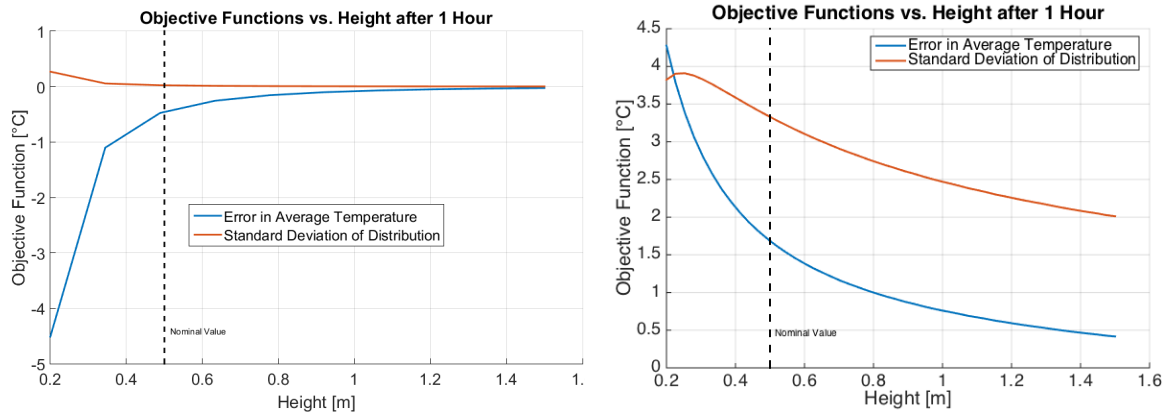

(a) Analytical Model **(b)** Numerical Model

Figure 21: Effects of Variation of Height in Both Models

This figure mirrors very closely the result from the width variation, as both the width and height are the two dimensions through which the water is assumed to not flow or diffuse heat.

Finally, a simultaneous variation of all three dimensions is implemented. This "volume factor" is the ratio of volume to nominal volume. The results from this analysis are shown in Figure 22 below.

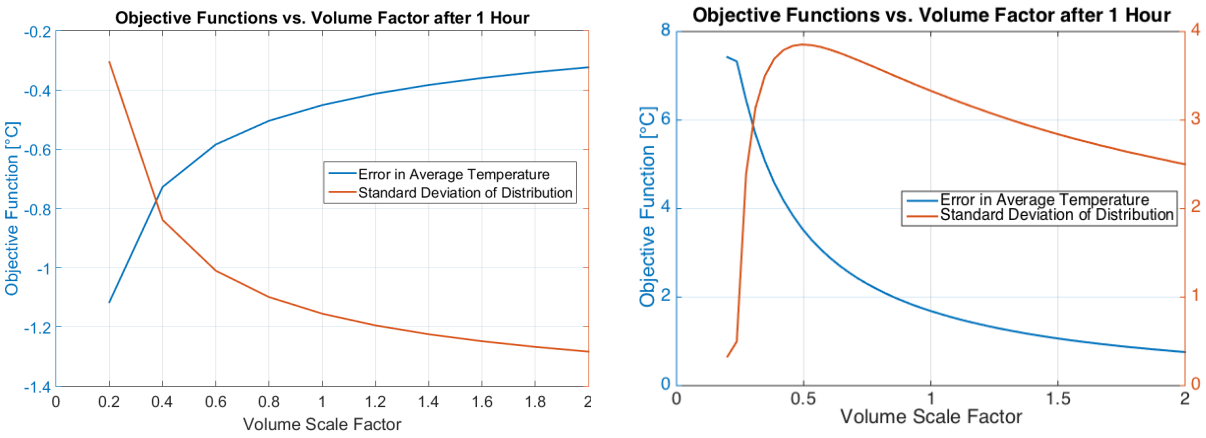

(a) Analytical Model **(b)** Numerical Model

Figure 22: Effects of Variation of Volume in Both Models

These results reflect those of the height and width variations, which suggests that height and width are more significant parameters in describing the temperature distribution throughout the bathtub, because they correlate strongly with convective heat losses to the air.

The results from this subsection emphasize the strength of the numeric model over the analytical model due to the importance of the bulk motion of the water, which is only accounted for in the numerical model.

8.3 Effect of Adding Soap

If Joe were to use a bubble bath additive or soap, this would change the thermal properties of the water which would ultimately result in a change in thermal diffusivity. The primary ingredient of soap is sodium stearate which is also used in bubble bath solutions. The density of sodium stearate is 1020 kg/m^3 [8]. This density is nearly identical to that of water and as such should have little to no effect on the density of the water when dissolved especially as the soap to water ratio would be small in a full bath. By adding a solute such as sodium chloride to pure water, the thermal conductivity decreases as solute concentration increases[9]; it is a reasonable assumption that adding sodium stearate results in a similar effect.

Overall, the approximately inconsequential addition of sodium stearate to water in realistic concentrations slightly reduces the diffusivity of the water. To perform a sensitivity analysis of this parameter, a wide range of diffusivities (a full order of magnitude about the standard diffusivity of water) was tested. This wide range was used to in order to show a noticeable change in solution behavior. Final temperature distributions after one hour are

shown for various values of thermal diffusivity below with the figure at right magnifying the area of interest.

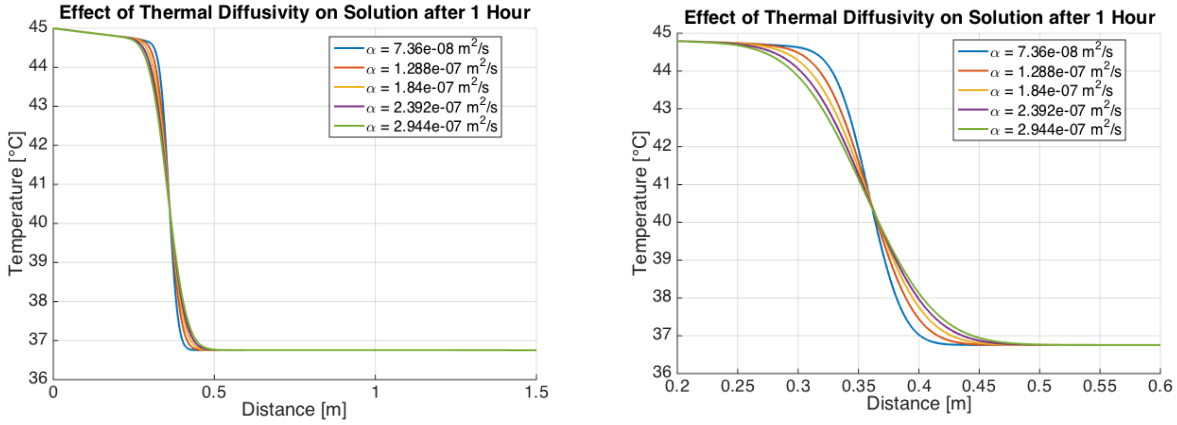

(a) Varied of Diffusivity over Full Length

(b) Magnified Variations of Diffusivity

Figure 23: Effects of Variation of Thermal Diffusivity in Numerical Model

The thermal diffusivity has very little effect on the solution, especially considering the wide range of thermal diffusivities tested. This continues to support the hypothesis that the heat transfer is primarily due to bulk flow and not diffusion. By examining the Péclet number (Pe)[10], we can confirm this hypothesis. The Peclet number is the ratio of the convective transport rate to the diffusive transport rate, as shown below with our nominal values.

$$\text{Pe} = \frac{vL}{\alpha} = \frac{(1.2 \times 10^{-4}\ \text{m/s})(1.5\ \text{m})}{1.472 \times 10^{-7}\ \text{m}^2/\text{s}} \approx 1223 >> 1 \tag{56}$$

This large ratio confirms that diffusion effects are negligible in comparison with bulk motion effects, due to the low thermal diffusivity of water. From this point onward, only the numerical model will be considered as the analytical model fails to capture the most important mechanism of heat transfer: bulk fluid motion.

8.4 Effect of Varied Input Temperature and Flow Rate

Up to this point, sensitivity analyses have been presented for the physical parameters of the system: the dimensions/shape of the bath and the thermal properties of the water in the bath. The next set of sensitivity analyses will be focused on the parameters that can vary during the course of the bath: the input water stream and the properties of Joe himself. First we analyze the effect of changing the input water temperature and mass flow rate. The results from this analysis are shown below in Figure 24.

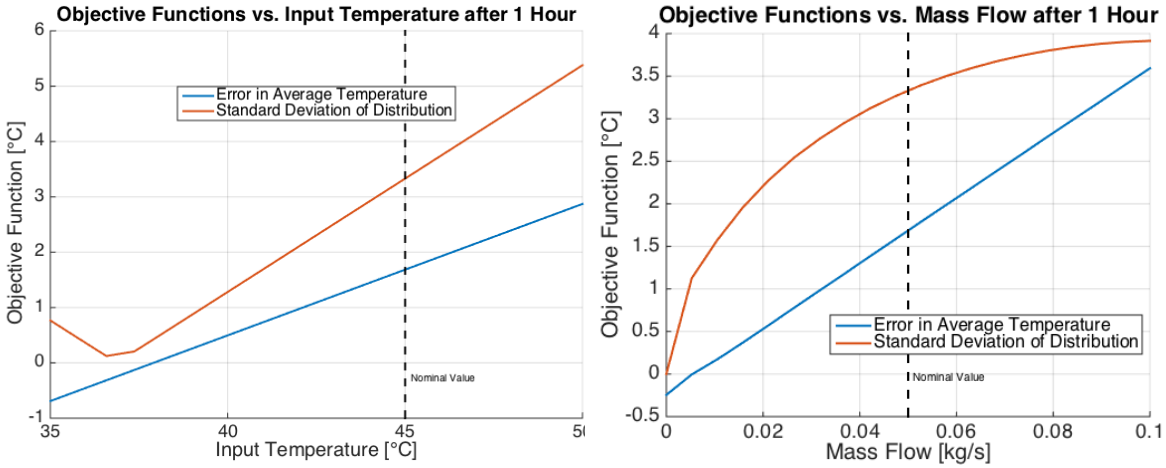

(a) Variation of Input Temperature **(b)** Variation of Mass Flow Rate

Figure 24: Effects of Varied Input Temperature and Mass Flow at Input

Increasing either parameter corresponds to an increase of net energy in the system. Another important result is that a large flow rate will result in a more uniform distribution when compared with a high temperature inlet. This is because increasing the mass flow rate increases the convective term, which is more efficient than the diffusion. The x intercepts of the blue lines on each plot represent important values, namely the input temperature or mass flow required to add the correct amount of heat to the system to maintain the objective temperature.

Heat maps for a low (35°C) and high (50°C) inlet temperature are shown below to further validate the model.

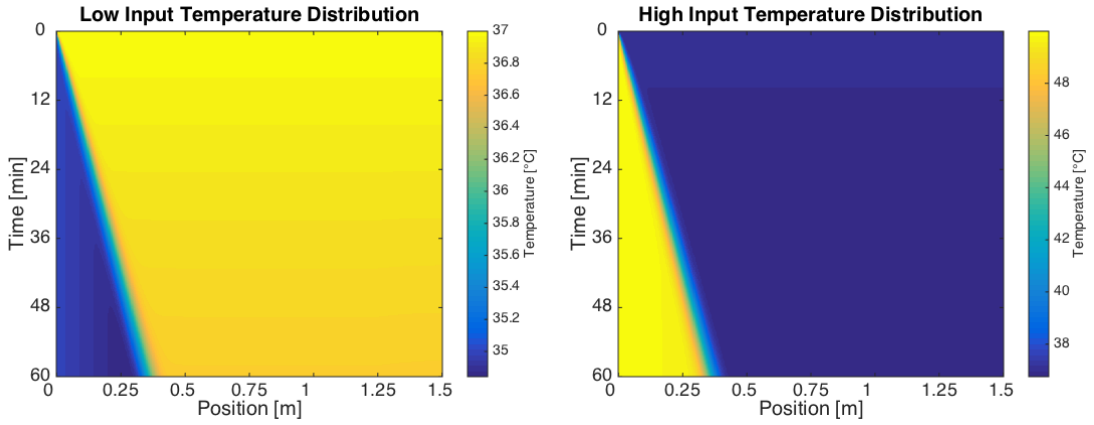

(a) Low Input Temperature **(b)** High Input Temperature

Figure 25: Heat Map Comparison of Input Temperature Effect in Numerical Model

In both cases, the input water convects across the bath, with a slight diffusive effect present at the boundary between the input water and the initial water. The rate of bulk fluid motion is clearly visible as the diagonal line of large temperature gradient. Similarly, heat maps for zero mass flow and high mass flow (twice the nominal value) are shown below.

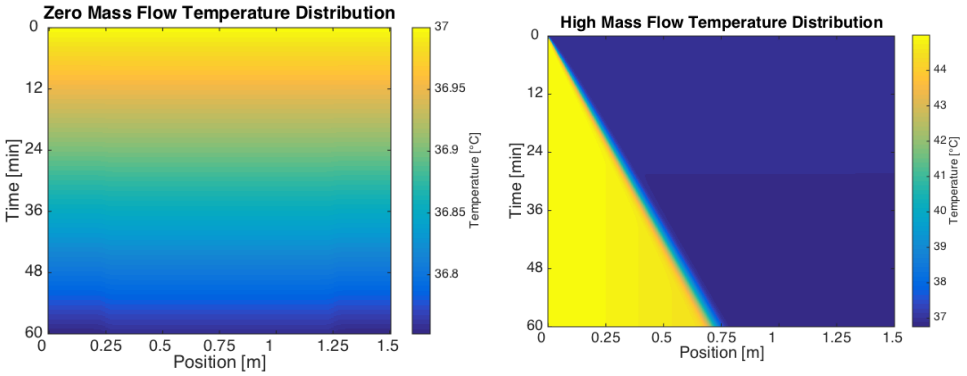

(a) Zero Mass Flow Rate **(b)** High Mass Flow Rate

Figure 26: Heat Map Comparison of Mass Flow Rates in Numerical Model

In the zero mass flow case, the water temperature is uniform at any given time, but is slowly cooling due to thermal energy loss into the surroundings. In the high mass flow rate case, the increased rate of bulk fluid motion can be seen. After one hour, the high temperature water has moved farther into the bath.

8.5 Effect of Varied Size and Position of Bather

The final parameter to be analyzed in the simulation of the bathtub is Joe himself. Any given bather may have different properties, such as width, length, temperature, or ability to transfer heat to or from the system.

These possible variations in parameters will be broken into two different categories: physical dimensions of the bather and the thermal properties of the bather. Below are the plots of the effects of the geometric parameters on the objective functions.

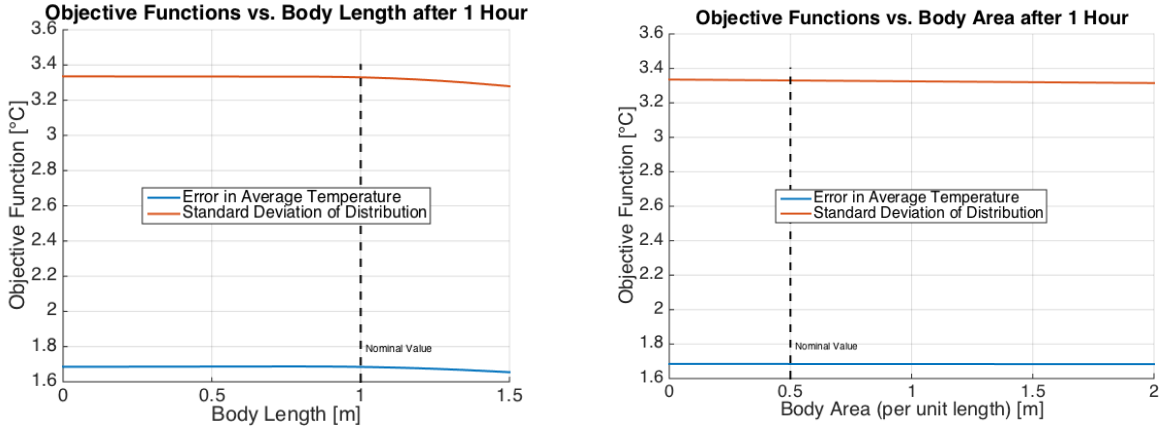

(a) Effect of Body Length **(b)** Effect of Body Surface Area

Figure 27: Impact of Body Shape and Size on Objective Functions

Neither Joe's body length nor his circumference (surface area per unit length) have a significant effect on the temperature distribution. It is only for a very long body (near the length of the bath itself) that uniformity and average temperature error are slightly improved. These results suggest that the physical dimensions of the bather have a negligible effect on the objective functions, due to the fact that the body temperature is close to the temperature of the bath.

The effects of the Joe's thermal parameters are shown below.

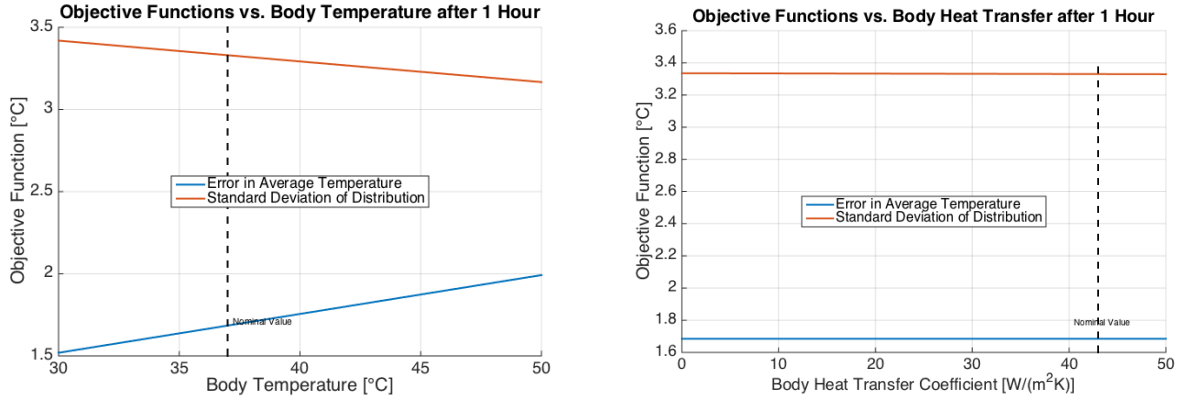

(a) Effect of Body Temperature

(b) Body-Water Heat Transfer Coefficient

Figure 28: Impact of Thermal Properties of Body on Objective Functions

The first sub-figure shows that Joe's body temperature has a slightly more significant impact than the geometry, which makes sense considering the difference in temperature between Joe and the water. However, it is important to note that this sensitivity is shown over a large range. The heat transfer coefficient has little to no impact, once again due to the small temperature difference between Joe and the water.

9 Control Theory and Implementation

In this section, we examine the implementation of closed-loop control for the regulation of average temperature and temperature uniformity. Up to this point, we have only considered cases where the initial and objective temperatures are the same. This correlates to Joe being proactive and attempting to mitigate the heat loss before the temperature drops noticeably. Now, we consider the case where the initial temperature is uniform, but noticeably lower than the objective, a potentially more realistic application.

9.1 PID Control Theory

Joe's ultimate goal is to experience a bath that is both maintained at a desired temperature and uniform in temperature through the water. Up to this point, many of the parameters that influence the response of the temperature distribution have been analyzed. However, the time dependence of these sensitivities has not been considered. We wish to develop a

time dependent strategy for Joe to achieve a uniform bath at the objective temperature using Proportional-Integral-Derivative (PID) control.

The first portion of the control system is designed only to achieve and maintain the objective temperature by using the average temperature metric detailed previously. Proper distribution can only take place if the correct amount of energy is already present in the system. As the net amount of heat in the bath is directly controlled by the faucet, this segment of the control system will focus on optimization of the inlet temperature and flow rate of the water from the faucet.

PID control is implemented through the selection of the *gains* associated with each component of the control. Below in Equation 57 is the general gain equation of a PID controller as a function of the objective $\overline{u}(t)$ with variable gains K for each stage, where $f(t)$ represents the calculated forcing (input).

$$f(t) = K_p\overline{u}(t) + K_i \int_0^t \overline{u}(\tau)d\tau + K_d\frac{\partial\overline{u}(t)}{\partial t} \tag{57}$$

Each of the three components of a PID controller corresponds primarily to a specific response of the system. The proportional control element is based on the difference between actual temperature and objective temperature; this control is what physically drives the system to the objective. The integral component defines the response on accumulated error from the objective instead of current error, decreasing the rise time and removing the steady state error from the system. The derivative component predicts the response error based on the temporal derivative of the response, damping any oscillations.

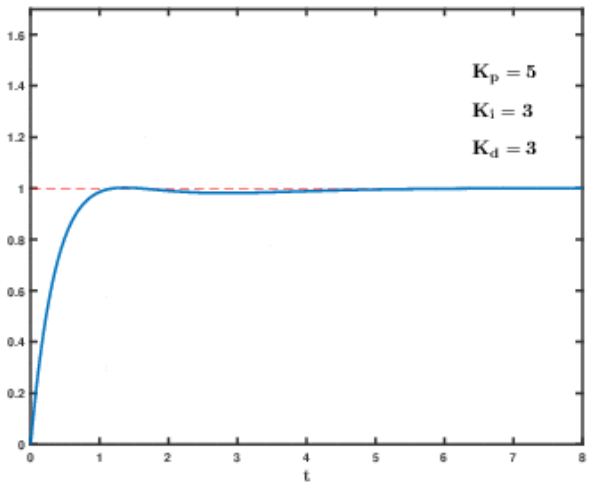

Figure 29: Illustration of Properly Tuned PID Controller[11]

At right is an image of the effects of each of the three components of a PID controller with properly tuned gains. Properly tuning each gain results in the optimal responses described: a small rise time with minimal oscillation and no steady state error.

9.2 Implementation of PID Control in Numerical Model

PID control was implemented in the numerical model by simply specifying the forcing as a function of $\overline{u}(t)$, as shown in Equation 57. In particular, we set

$$f(t) = \dot{m}(u_{in} - u(x = 0, t)), \tag{58}$$

a term in the inlet Neumann condition.

In addition, the gain coefficients needed to be determined. These gain coefficients should weight the response with the ultimate goal of achieving a response with minimal rise time,

little to no overshoot, and long term stability. These desired responses have strong grounding in the reality of the physical system. The rise time is desired to be short so that Joe does not have to wait long for his bath to reach the objective temperature. Too much overshoot could result in Joe being burned, and is thus not desired. Finally, long term stability reflects the maintenance of the desired temperature over the course of the entire bath duration.

There are many methods for determining optimal gains, including PID control software and algorithms such as the Ziegler-Nichols tuning process, but due to the lack of a well defined transfer function in the numerical approach, neither option is applicable and manual tuning is required.

We manually tuned our gains in order to obtain a roughly optimal response. In no way are the following system responses the result of optimal gains; much more tuning would be required for such an optimization. Below, we present the system response using only proportional control, starting at 30°C and attempting to reach 37°C.

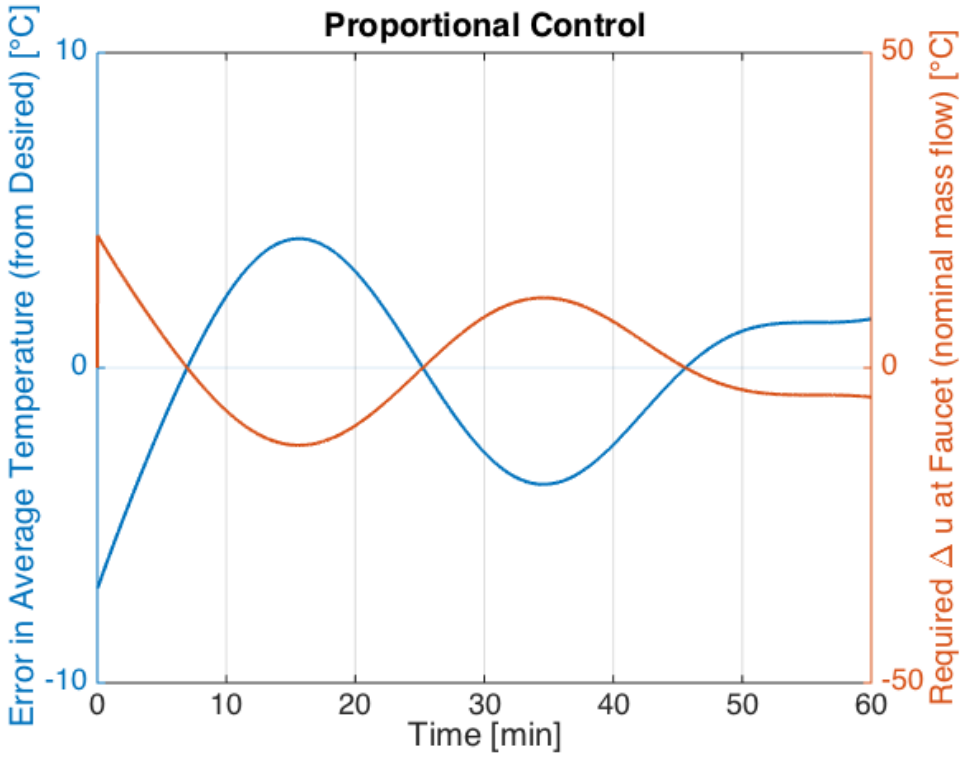

Figure 30: Effect of Proportional Control

There are noticeable oscillations in the objective function (the blue line) and there is an overshoot of about 4°C. Since the forcing is a function of both mass flow and inlet temperature, we fix mass flow and present the result as the required Δu (the red line). The Δu peaks at around 20°C, meaning that the inlet water temperature must be 20°C hotter than the current water temperature at the inlet.

Using full PID, the results from the same analysis are shown below in Figure 31.

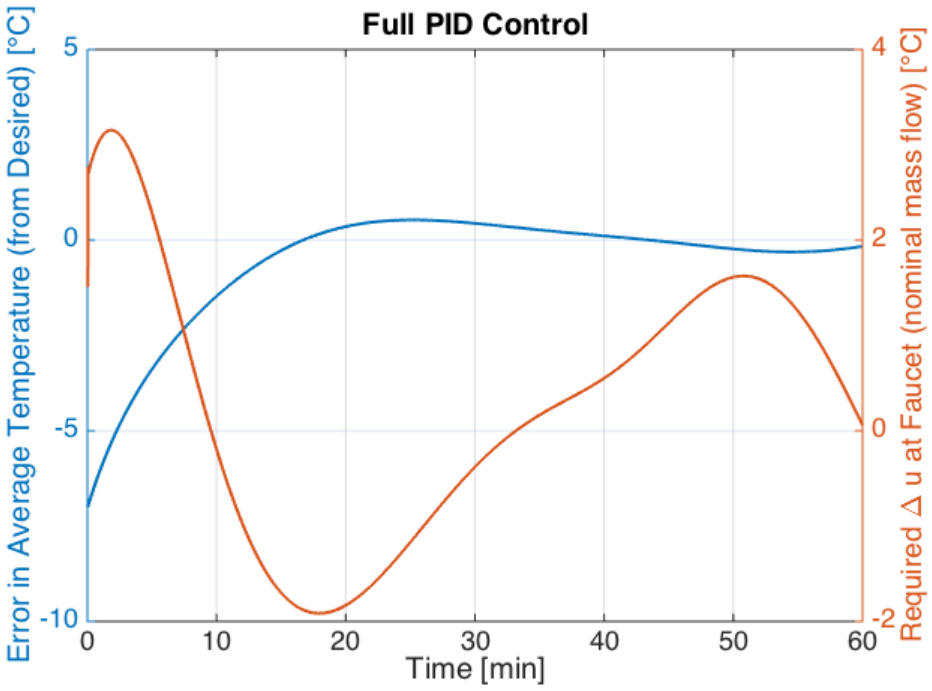

Figure 31: Optimal Control of Average Bath Temperature

The objective function is driven to nearly zero, as desired. More importantly, the response is achieved with a relatively short rise time, minimal overshoot, and maximal oscillation of less than a degree. The associated forcing function is more reasonable, requiring a maximum Δu of about 3°C.

9.3 Control of Uniformity of Water Temperature Distribution

With the average temperature of the water driven to the objective temperature using PID control, the only remaining factor is the uniformity of the temperature distribution. The method of maintaining uniformity is very simple: instead of adding heat from the faucet to the bathtub at $x = 0$, we evenly distribute the hot water over the whole bath. Physically, this method corresponds to Joe continuously redirecting the water from the faucet, using a cup or another redistribution system.

Logically, it makes sense to evenly distribute the heat throughout the bathtub. Assuming an initial temperature of 37°C and an objective temperature of 37°C (which corresponds to Joe being proactive about the heat loss in the bath), this logical argument is easily verified. In Figure 32 below, we show the objective functions vs. inlet temperature, where the heat is being distributed evenly and the mass flow is fixed. We also show the heat map using the optimized input temperature.

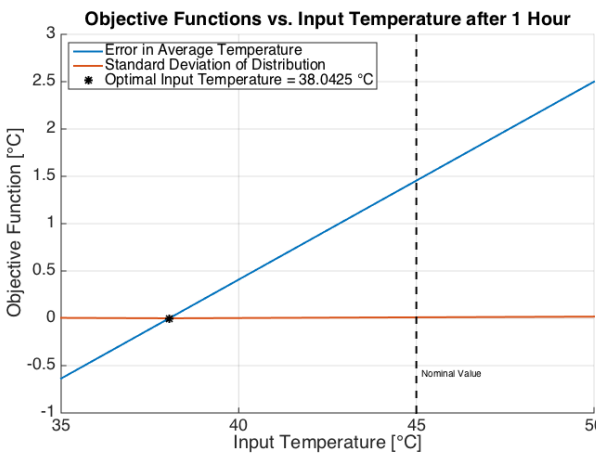

(a) Optimal Input Temperature

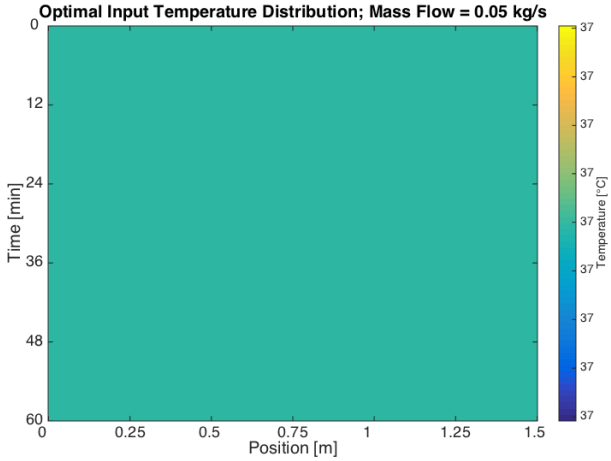

(b) Heat Map of Optimized Uniformity

Figure 32: Determination of Optimal Input Temperature with Prescribed Flow Rate

The uniformity objective function (the red line) is maintained at zero which confirms the hypothesis that uniform heat distribution is most effective. The heat map demonstrates that using the optimal input temperature for the given mass flow rate results in a perfect bath. The same results are shown in 33 below, this time varying the mass flow with a fixed inlet temperature.

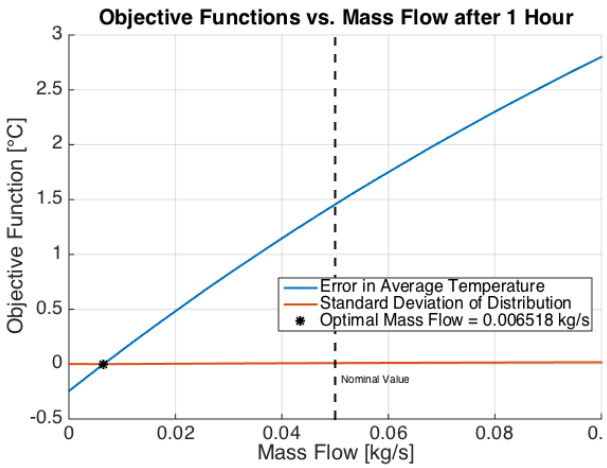

(a) Optimal Mass Flow Rate

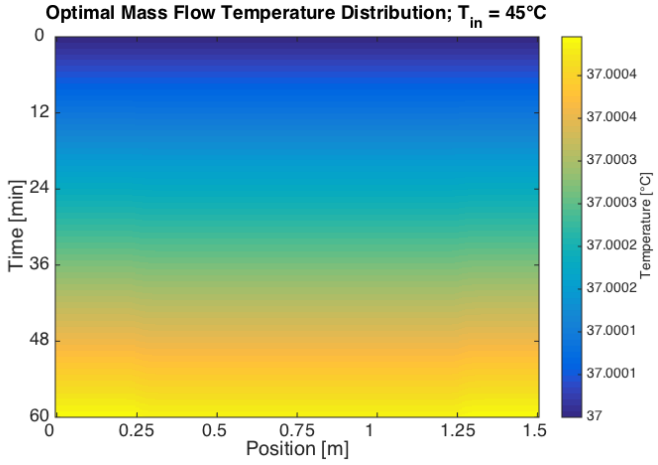

(b) Heat Map of Optimized Uniformity

Figure 33: Determination of Optimal Mass Flow Rate with Prescribed Nominal Input Temperature

Just as before, there exists an optimal mass flow, and using this mass flow with uniform distribution, a perfect bath is once again achieved.

9.4 Final PID Control with With Manual Heat Distribution

We close with a simultaneous consideration of average temperature (PID) control and uniformity control. Up to this point, we have analyzed these control methods separately and under different initial conditions, but to complete our model of the problem it is essential that we implement them simultaneously. The initial condition will be a 30°C uniform bath, and the objective will be 37°C, accurately modeling Joe's realization that his bath has become cold.

The combined model will effectively implement the two control methods by using PID control to determine required temperature of the incident water (given a constant nominal mass flow rate), and using intelligent input water redistribution to maintain uniformity. The intelligent redistribution was determined by tweaking the locations at which the input water is distributed. Ultimately, it was determined that distributing inlet water over the region from $x = 0$ m (the faucet) to the location that the body starts, $x = 0.25$ m for the nominal case, is optimal. This allows the body heat to convect downstream and the inlet heat to warm the water upstream of the body.

After manually tuning the gains and implementing full PID in addition to intelligent inlet water distribution, the following results are obtained.

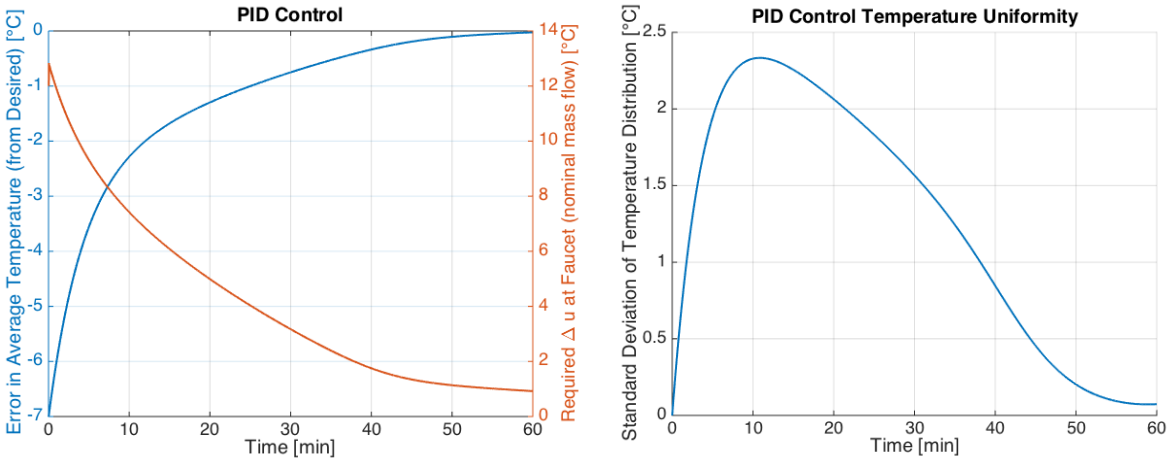

(a) PID Control with Manual Heat Distribution **(b)** Uniformity over Time

Figure 34: PID System Response Using Intelligent Heat Distribution

On the left, the average temperature objective function is shown to rise to zero relatively quickly with no overshoot, an optimal result. Additionally, the required Δu with a nominal flow rate is physically reasonable. On the right, the temperature uniformity is shown to initially increase (due to Joe's body) but settle to zero as the inlet water distribution begins to have an effect.

The heat map corresponding to this control is shown below in Figure 35.

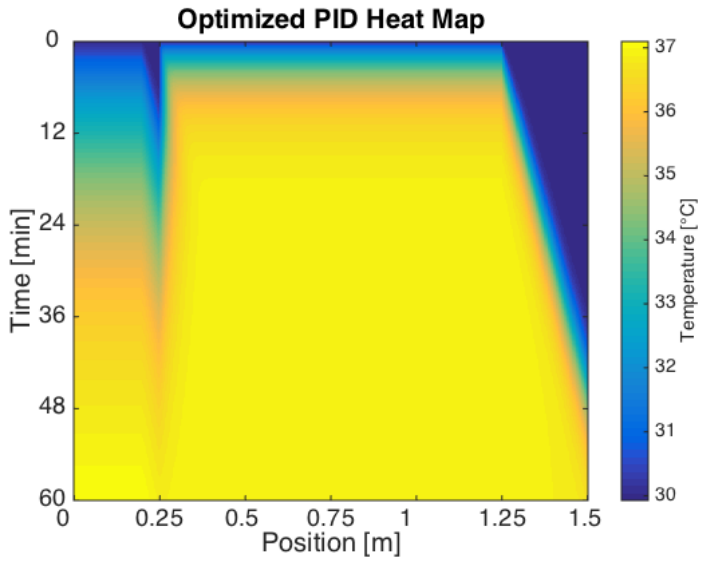

Figure 35: Heat Map of PID System Response Using Intelligent Heat Distribution

This result illustrates the optimal strategy that Joe can take to increase his bath temperature to his objective while keeping the temperature distribution uniform and only using a nominal trickle of water. He should use PID control to vary the input temperature and simultaneously use a cup or other redirecting device to continuously distribute the inlet water over the region of the bathtub that is upstream of his body.

10 Final Remarks

We have now completed our mathematical modeling of the bathtub. In this section, we will conclude our paper, commenting on each of our models and presenting ideas for future work.

10.1 Strengths and Weaknesses of Solution Models

Each of our final models had very specific strengths and weaknesses. Below are a list of strengths and weaknesses for the three models developed in this report: the steady state uniform model, the analytical model of heat diffusion, and the numerical model of the convection-diffusion equation.

Steady State, Uniform Temperature Model

Strengths:

- The implementation is straightforward and the derivation is based solely on thermodynamics.
- The results can be used to qualitatively predict the results of more complicated models.

Weaknesses:

- No spatial or temporal dependence is considered.

Analytical Solution Model

Strengths:

- Time dependent boundary conditions and both a spatially and temporally dependent forcing function (heat source) can be effectively modeled.
- The boundary conditions can be customized to reflect the physical system.
- The model yields a highly accurate analysis of characteristic transient solutions over one dimensional space due to heat diffusion.

Weaknesses:

- Bulk flow of the fluid is not modeled.
- The simulation implementation proved challenging when considering various types of boundaries and sources.

Numerical Convection-Diffusion Model

Strengths:

- Solution incorporates effects of both convection and diffusion for a realistic fluid thermodynamic simulation.
- Time dependent boundaries and a spatially and temporally dependent heat source can be customized.
- The straightforward implementation of simulations allows for a variety of tests of parameter sensitivity analyses as well as the implementation of control.
- The numerical approach allows for the possibility of expansion of the simulations into a multidimensional model.

Weaknesses:

- The foundational mathematics of this numerical implementation are highly involved.

The greatest overall strength of all of the models was their generality. This allowed for a wide range of parameter customization, from dimensions of the bath, types of boundaries enforced on the system, heat transfer coefficients, effects of Joe in the system, and final control application. The main weakness of our models is that they only consider one-dimensional heat flow. In reality, the thermal-fluid effects in a bathtub will be largely three-dimensional.

10.2 Future Model Development

As discussed in the weaknesses of the models, many possibilities exist for the development of a more precise model. In the future, a more comprehensive and definitive model would be developed in the following ways:

- Expand the models to incorporate more detailed information through increasing the dimensionality of each model, more accurately reflecting a physical three-dimensional system.
- Conduct experimental trials and extensive research to ensure the accuracy of certain physical parameters, such as transfer coefficients for humans or precise effect of soluble materials on water's thermal properties.
- Apply geometry and coordinate transformations to explore the effect of various geometries on the system, such as cylindrical and trapezoidal geometries.
- Analyze the steady-state distribution of the thermal energy with high accuracy across three dimensions through implementation of Laplace's Equation, spatially dependent boundary conditions, and realistic heat loss.

10.3 Conclusions

In this paper, we modeled the temperature distribution in a bathtub in space and time in order to determine the most effective method of uniformly increasing the temperature. Three models were developed to describe this temperature distribution: a steady state uniform model, an analytical heat equation model, and a numerical convection-diffusion equation model. Ultimately, the numerical model proved most accurate because it alone took into account bulk fluid motion, the dominant heat transfer effect. Using this model and the analytical model, we conducted sensitivity analyses on different parameters to explore the effects of different bathtub geometries, the addition of soap, and other variations to the problem at hand. We also implemented PID control of the inlet water temperature and intelligent distribution of inlet water. By optimizing this process, we effectively developed a strategy for quickly re-heating the bath while maintaining uniformity. Overall, our model showed that well-tuned PID control combined with distributing the inlet water upstream of the bather proved to be the most effective strategy.

References

[1] "IAPWS Industrial Formulation 1997 for the Thermodynamic Properties of Water and Steam." International Steam Tables (2008): 7-150. Web.

[2] Cengel, Yunus A, and Robert H. Turner. Fundamentals of Thermal-Fluid Sciences. Boston: McGraw-Hill, 2001. Print.

[3] Boutelier, C., L. Bougues, and J. Timbal. "Experimental Study of Convective Heat Transfer Coefficient for the Human Body in Water." US National Library of Medicine (1977). PubMed.gov. Web. 31 Jan. 2016.

[4] Grigoryan, Viktor. "Inhomogeneous Boundary Value Problems." Math 12B, Fourier Series and Numerical Methods. University of California, Santa Barbara, 31 Jan. 2012. Web. 30 Jan. 2016.

[5] Haberman, Richard. Applied Partial Differential Equations: With Fourier Series and Boundary Value Problems. 5th ed. Upper Saddle River, NJ: Pearson Prentice Hall, 2013. Print.

[6] Ewa Majchrzak, ukasz Turchan, The Finite Difference Method for transient convection-diffusion problems, Scientific Research of the Institute of Mathematics and Computer Science, 2012, Volume 11, Issue 1, pages 63-72.

[7] Burden, Richard L, and J D. Faires. Numerical Analysis. Belmont, CA: Thomson Brooks/Cole, 2005. Print.

[8] "Sodium Stearate (CAS 822-16-2)." Sodium Stearate. Santa Cruz Biotechnology, 2007. Web. 31 Jan. 2016.

[9] Martinez, Isidoro. "Properties of Particular Solutions." UPM, Jan. 1995. Web. 1 Feb. 2016.

[10] "5. Advection and Diffusion of an Instantaneous Release." MIT.edu. Massachusetts Institute of Technology. Web. 1 Feb. 2016.

[11] PID Compensation. Digital image. PID Controller. Wikipedia, 28 May 2015. Web. 30 Jan. 2016.

Superior Products*:
Applied Mathematical Consulting Firm

Superior Products, L.L.C.*
Letter to International Society for the Promotion of Comfort and Cleanliness
2/1/16

As many of you are likely aware, there has been a singular problem facing avid bath users for many generations. Though we have come quite far as a society with the invention of running water, synthetic bathtub materials, and even advances in soap and shampoo solutions, the issue of keeping your bath at a comfortable temperature without pockets of cold or hot water has not been improved upon for generations.

Solutions range from self-circulating baths, expensive water jets, or even the deferring of a magnificent bath to a common shower, but an explanation has slowly presented itself to the difficulty shrouding this dilemma. The underlying factor of the cooling bath problem is a combination of being able to maintain heat within the bath over the course of your soak and also to distribute any hot water you introduce to the system. This is difficult due to the fact that water diffuses heat very poorly. Your relaxing afternoon bath is in reality a complex dynamical system, controlled by the physical phenomena of thermodynamics, heat transfer, and fluid mechanics.

Fortunately for the bathing community, a small percentage of our fellow bathers are not only aspiring to the ideals of cleanliness, but also ardently pursuing an understanding of applied mathematics. This question of the fluid dynamics of the bath tub has intrigued your friends here at Superior Products, and we have attempted to find a solution to the age old question of how to achieve the perfect bath.

Despite the daunting complexities of the common bathtub, the advent of modern computational methods and simulation tools has allowed for an extensive understanding of heat flow within the bath. Through careful studying of the heat loss from the bath, diffusion of energy from warm to cold regions, and the bulk flow of water from faucet to drain, a final solution to your issues has been found.

Ultimately, the solution involves precision control theory to define the optimal temperature of the incoming water at every given time of your bath. This temperature is chosen to achieve your ideal temperature quickly, without the risk of burning yourself. The second fundamental portion of the strategy is to spread the incoming water continuously over the surface of your bath as it enters through the faucet, possibly through the use of a cup or customized bathwater distribution device. Our generic solution can take into account any uniqueness in your specific bath, such as your desired bath temperature and your bathtub shape and size.

This simple yet refined strategy will ensure that your bath is always at the perfect, uniform temperature. Feel free to use whatever soaps, shampoos, or even enhanced bubble solutions to improve your bathing experience.

*This company is purely a work of fiction.